République Algérienne Démocratique et Populaire

Ministère de l'enseignement supérieur et de la recherche scientifique

Université colonel Hadj Lakhder-BATNA

Faculté des sciences

Département de physique

PRIMALAB

Mémoire

Présenté pour obtenir le diplôme de

Magister

Physique des rayonnements

Option : Physique Subatomique

Thème

Simulation des processus dynamiques des fluides astrophysiques

Par:

HElASSA Amel

Devant le jury :

D.Bahloul M.C. Univ. -Batna. Président

A.Bouldjedri Pr. Univ. -Batna. Rapporteur

S.Bougoul Pr. Univ. -Batna. Examinateur

J.Mimouni Pr. Univ. -Constantine. Examinateur

ABSTRACT

Fluid dynamics play a vital role in our understanding of the universe, where the fluid forces and theories control the largest range of astrophysical phenomena. Each type of flow we observe in terrestrial environments appears in the cosmos but with a huge scale. Recently, the research area of astrophysical hydrodynamics has rapidly developed due to the progress of observational data and numerical simulations by powerful computer resources.

The purpose of this magister thesis is to present some astrophysical phenomena treated with hydrodynamic equations, and we provide the necessary tools to understand their observation and evolution.

One of the most essential research topics in this domain is the accretion disks, because they are ubiquitously found around a variety of astrophysical systems, and they offer the opportunity to study their evolution and instabilities, for instance, the wide disk around young stellar objects (YSO) is an essential stage in the formation of stars and planets. The disk around active galactic nuclei (AGN) determines the emitted radiation from these objects, and in the case of interacting binary systems, they represent the channel for mass transfer between the two stars. Accretion disks are formed because the infalling matter onto the central object from the interstellar medium has a considerable angular momentum to settle into a disk's shape. Then, to remove this matter it must redistribute the angular

momentum by giving it up to the outer parts of the disk due to a various instabilities which develop in the disk, such as magnetorotational (MRI), gravitational, and hydrodynamical instabilities that cause turbulence in the disk. The issue of viscosity has been historically one of the most key issues to the understanding of accretion disk physics. In this thesis, we consider that the viscosity is generated only under the effect of turbulent instability, without taking neither magnetic nor gravitational field effect. Therefore, we study the structure of these disks with introducing a parameterization of the turbulent viscosity by the ?-disk model.

In the first chapter, we will illustrate the basic equations and theories of fluid dynamics that we will need in the study of accretion disks. A brief introduction of relativistic fluid dynamics is then give, with the computational codes which can be use to solve the relativistic hydrodynamical problems in astrophysics.

The second chapter is an overview of the basic dynamics and fundamental equations that determine the evolution of accretion disks. This is an essential first step needed to embark on the discussion of the more complex phenomena associated with them. Also, it represents the beginning of the study by the case of Keplerian disks with constant viscosity.

The focus of the third chapter is on the study of steady state solution of both thin and thick disks, where we applied the equations of the first case to disk around a white dwarf, in order to get more information about their properties in this case.

In the last chapter, we have used the concept of turbulent viscosity to treat time-dependent solutions for thin accretion disks, which allows us to understand

their evolution with time.

ACKNOWLEDGMENTS

I deeply express my great gratitude and limitless respect and esteem to Mr.A Bouldjadri, professor at the University of Batna and my thesis reporter. Thousands of thanks for your continuous help, your precious advice and real confidence, thank you sir.

I would like then to thank all the jury members Mr.D Bahloul, Mr. S Bougoul and Mr.J Mimouni for their important participation, their time and help.

I thank my true and dearest friend Ms. Z Amel for her help and her support. "Real friends those who are two, but feel as one".

Finally, i thank all those who helped me and offered me much time and care.

CHAPTER 1

Elements of fluid dynamics

Fluid dynamics play an important role in our understanding of the wide universe, from the stars, interstellar medium, intergalactic medium, internal structure of giant planets, jets, stellar winds, to accretion disks. To identify the dynamical behaviour of fluids, we need to have a set of five equations of conservation; the mass conservation, the three compenents of momentum conservation and the energy equation.

These fundamental equations derived by considering the fluid as a continuous medium, the macroscopic description, which is realized when the macroscopic length scale L of the system is very large compared to the mean free path λ of the particles; $L \gg \lambda$.

In this thesis, the equations of conservation are written with *the Eulerian description*, where the fluid properties vary in time at a fixed spatial position, as if we observe a fixed point in space as time proceeds. The Eulerian time-derivative of any measurable quantity f is $\partial f/\partial t$ evaluated with a fixed position. The other approach which can formulate the equations of conservation is *the Lagrangian description*. In this approach the fluid properties vary at a point that moves with the fluid. The Lagrangian time-derivative of any measurable quantity f is $\frac{Df}{Dt} = \frac{\partial f}{\partial t} + (u.\nabla)f$, where u is the velocity field.

In this chapter, we present some bases of fluid theory that we will need in our

following study. We first define the principal conservation laws (mass, momentum and energy conservation). Then, we describe two simplifying models (incompressible and polytropic), they are used in our next calculations. We next define two dimensionless numbers (Reynolds and Mach number) and the viscous forces which play an important role in the transport of material in the disks. As turbulence play a major role in the matter transport in accretion disks, we will describe some fundamentals of this theory. Finally, we try to give an introduction about the relativistic astrophysical fluids.

1.1 Conservation laws

To completely characterize the state of any fluid in motion, we need to determine five field functions which are the three components of velocity field $v(r,t)$, the pressure $p(r,t)$ and the mass density $\rho(r,t)$. Here we will write the conservation laws without mentioning the stages of their derivation, we will indicate only the meaning of each term.

1.1.1 Conservation of mass (Continuity equation)

The continuity equation is one of the most essential conservation laws, used in the analysis of flowing fluids. It is a differential equation form, it expresses the mass conservation of moving fluids. The principle of this conservation law states that the mass is neither created nor destroyed, it only changes into a different form of matter, which means that for any control volume ($Fig\ 1-1$), the mass flow rate entering equals the mass flow rate leaving in addition to the increase of mass in

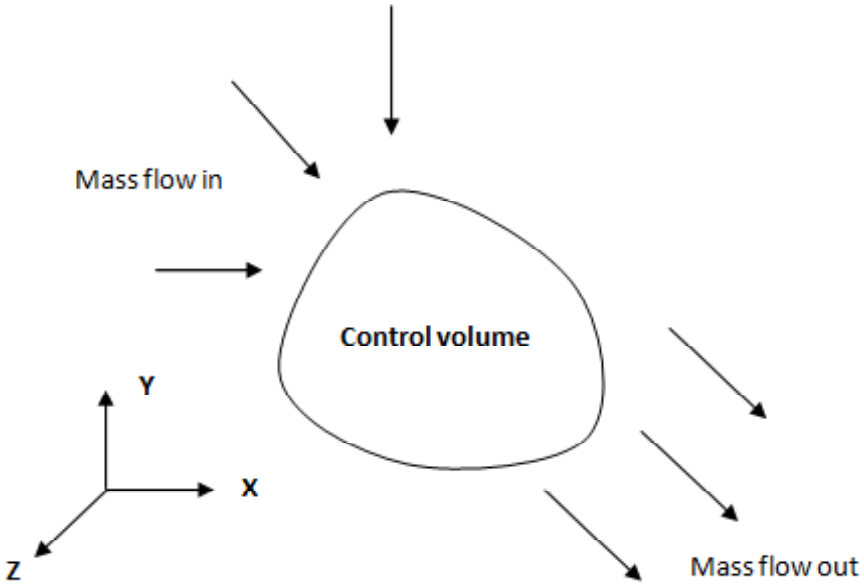

Figure 1.1: Fluid flow in a control volume.

this volume, and for any steady flow, the mass flow rate entering equals the mass flow rate leaving.

The general form of the mass conservation law is

$$\frac{\partial \rho}{\partial t} + \overrightarrow{\nabla}.(\rho \overrightarrow{v}) = 0 \tag{1.1}$$

where v is the fluid velocity, the term $\overrightarrow{\nabla}.(\rho \overrightarrow{v})$ is the divergence of the mass flux density. For steady flows, the density ρ is not a function of time and thus the continuity equation is simplified to

$$\overrightarrow{\nabla}.(\rho \overrightarrow{v}) = 0 \tag{1.2}$$

1.1.2 Conservation of momentum (Navier-Stokes and Euler equations)

The principle of momentum conservation law states that, for any control volume, the momentum is constant if there are no external forces acting on this volume, which means that the rate of change of momentum is balanced by the forces applied on it. There are two types of forces can affect the control volume, *body* and *surface* or *contact forces*. The first are the forces that have the largest influence on all the volume particles. The most important body force is that due to gravity. The second forces arise due to pressure or viscous stresses, they only affect one particular surface of the control volume.

Navier-Stokes equations express the equality between the quantity of acceleration, and the external forces acting upon a unit volume. They are calculated by the application of Newton's second law of motion on an element of fluid, with the assumption that the forces exerted on the fluid element are pressure, volumic forces, gravity and viscous stresses. The general form of this equations is

$$\rho\frac{\partial v_i}{\partial t} = -\frac{\partial p}{\partial x_i} - \rho v_j\frac{\partial v_i}{\partial x_j} + \rho g + \frac{\partial \sigma'_{ij}}{\partial x_j} \tag{1.3}$$

with p the pressure, g the acceleration due to gravity, σ'_{ij} the viscous stress tensor (see section 4), i represents the component and j the direction. Substituting with expression of σ'_{ij}, equation (1.3) becomes

$$\rho\left(\frac{\partial v_i}{\partial t} + v_j\frac{\partial v_i}{\partial x_j}\right) = -\frac{\partial p}{\partial x_i} + \rho g + \frac{\partial}{\partial x_j}\left\{\eta\left(\frac{\partial v_i}{\partial x_j} + \frac{\partial v_j}{\partial x_i} - \frac{2}{3}\delta_{ij}\frac{\partial v_k}{\partial x_k}\right)\right\} + \frac{\partial}{\partial x_j}\left(\xi\frac{\partial v_k}{\partial x_k}\right) \tag{1.4}$$

where η and ξ are coefficients of viscosity. They are both functions of pressure and temperature, but in many practical cases they may be considered as positive

constants $\eta > 0$, $\xi > 0$. The vector form of this equation is

$$\rho\left[\frac{\partial\overrightarrow{v}}{\partial t}+(\overrightarrow{v}.\overrightarrow{\nabla})\overrightarrow{v}\right]=-\overrightarrow{\nabla}p+\rho\overrightarrow{g}+\eta\triangle\overrightarrow{v}+\left(\xi+\frac{1}{3}\eta\right)\overrightarrow{\nabla}.\nabla\overrightarrow{v} \tag{1.5}$$

Euler equations correspond to Navier-Stokes equations with the absence of viscosity. They are the equations that describe the motion of inviscid fluid, given by

$$\rho\left[\frac{\partial\overrightarrow{v}}{\partial t}+(\overrightarrow{v}.\overrightarrow{\nabla})\overrightarrow{v}\right]=-\overrightarrow{\nabla}p+\rho\overrightarrow{g} \tag{1.6}$$

Since Navier-Stokes and Euler equations are non-linear, partial and differential, they cannot be solved exactly, so they are commonly used in computational fluid dynamics. These equations can be simplified, a number of approximations make them easier to solve.

1.1.3 Conservation of energy (Energy equation)

The energy equation is a partial differential equation discribes the dynamical state of real fluid. It states that energy in a closed system cannot be created or destroyed, it can only be changed in form, indicates that the total change in fluid energy within the control volume equals the net thermal energy transferred, in addition to the rate of work done by external forces, so the energy equation is written on the form

$$\frac{\partial}{\partial t}\left[\rho\left(\frac{1}{2}v^2+\varepsilon\right)\right]+div\left[\rho v\left(\frac{1}{2}v^2+w\right)\right]=div\left[v.\sigma'\right]+\rho vg-div\left[q\right] \tag{1.7}$$

The left hand side of this equation represents respectively the change in total fluid energy per unit volume plus the net transfer of energy through the control

volume, or the flux of energy due to the simple mass transfer by the effect of the fluid motion, where ε being the internal energy per unit mass, w being the heat function. First term in the right hand side represents the rate of work done by the surface forces per unit volume, that corresponds to the multiplication of velocity with viscous stress. The second term is the rate of work done by the gravity force per unit volume, and the last term is the net thermal energy transferred into the control volume, where q is the heat flux density due to thermal conduction, given as

$$q = -kgradT \tag{1.8}$$

k is constant, called the thermal conductivity, it is always positive because the thermal conduction causing a direct molecular transfer of energy from points of high temperature to points of low temperature. In the case of ideal fluid, we eliminate the effect of viscous sterss and thermal conduction, the energy conservation law is written

$$\frac{\partial}{\partial t}\left(\frac{1}{2}\rho v^2 + \rho\varepsilon\right) = -div\left[\rho v\left(\frac{1}{2}v^2 + w\right)\right] \tag{1.9}$$

1.2 Simplifying models

1.2.1 Incompressibility

In fluid mechanics, a fluid is said to be incompressible if a volume element is neither dilated nor compressed when moving with the flow. In other words, the fluid moves with negligible changes in density (ρ=constant). In reality no fluids are truly incompressible, because such fluids can have an increasing density

through the application of sufficient pressure. This is a very useful simplifying assumption because the treatment of incompressible flows is much easier than that of the compressible ones.

In the incompressibility limit, the mass continuity equation is simplified to a volume continuity equation, as follows (with ρ=constant)

$$\overrightarrow{\nabla}.\overrightarrow{v} = 0 \tag{1.10}$$

which gives that the divergence of velocity field is zero everywhere.

And Navier-Stokes equation becomes (with $\nabla \overrightarrow{v} = 0$),

$$\rho \left[\frac{\partial \overrightarrow{v}}{\partial t} + (\overrightarrow{v}.\overrightarrow{\nabla})\overrightarrow{v} \right] = -\overrightarrow{\nabla p} + \rho \overrightarrow{g} + \eta \triangle \overrightarrow{v} \tag{1.11}$$

1.2.2 polytropic

A polytropic simplification method is to give a simple relation for the state equation, where the name polytropic is derived from the polytropic process. This latter is a thermodynamical reversible process, it obeys a relation used to accurately characterize processes of compression or expansion of gases (generally regarded as ideal gases), and in some cases, possibly liquids and solids. The polytropic relation can be written in different forms, one of the most commonly used expression is to give the variation of the pressure and the volume as

$$PV^n = K \tag{1.12}$$

where P the pressure, V the volume, n the polytropic index (a real number), and K is the polytropic constant. The index n depending on the process type, some values of n correspond to particular states of matter, which are

•if $n = 0$, so $P = K$, it is an isobaric process (process with constant pressure).

•if $n = 1$, so $PV = K$, it is an isothermal process (process with constant temperature).

•if $n = \gamma$, so $PV^{\gamma} = K$, it is an adiabatic process for a perfect gas (process with no heat transferred), where $\gamma = C_p/C_v$ is the adiabatic index defined as the ratio of specific heat at constant pressure to specific heat at constant volume.

•if $n = \infty$, so $P^{\frac{1}{n}}V = K^{\frac{1}{n}}$, it is an isochoric process (process with constant volume).

•if $n < 0$, an explosion occurs.

The equation of a polytropic process can be written in a different other form than (1.6). In stellar models, it is more appropriate to use the relation that gives the variation of the pressure with density, which is

$$P = K\rho^{1+\frac{1}{n}} \tag{1.13}$$

In this case the polytropic index n takes different values correspond to the nature of the stellar object matter. for a fully ionized, degenerated and nonrelativistic gas, n takes the value $3/2$ (it is a good value for the study of the degenerate stars cores as white dwarfs, red giant stars and giant gaseous planets), $n = 3$ is the case of gas where the radiation pressure is the dominant, as stars in main sequence and the Sun, for diatomic molecular gases, n is equal to $5/2$.

In astrophysics, this simplification method plays an important role in the study of stellar structures, it helps to define the internal structure of stars by finding a simple solution for the stellar density, similar to the solution which can be found by a computational methods.

1.3 Dimensionless numbers

1.3.1 Reynolds number

The experimental study of the turbulent flow started with Reynolds expreriences on the different flow regimes in pipes. He noted that the nature of the flow depends on the fluid velocity v, its viscosity ν and the diameter d of the pipe. So, he introduced the dimensionless number $\Re$, called *Reynolds number*

$$\Re = \frac{vd}{\nu} \tag{1.14}$$

This dimensionless number plays the role of a control parameter because it helps to identify the type of the flow. Laboratory experiences indicated a critical Reynolds number $\Re_{cr}$ takes different values for each type of flow, ranging between 10 to 100 [$Lan87$]. For sufficiently small Reynolds number ($\Re < \Re_{cr}$), the flow exhibits small instabilities (laminar case). For sufficiently large Reynolds number, the flow becomes turbulent.

1.3.2 Mach number

The dimensionless Mach number is a flow property, it is defined as the ratio

of the speed of an object to the sound speed in the surrounding medium, so it is expressed as

$$\mathcal{M} = v/c_s \tag{1.15}$$

where v is the flow velocity, and c_s is the speed of sound. The Mach number is used in the analysis of fluid flow problems where the compressibility effects and shock waves are important. Therefore, it is important in the classification of flow regimes in which these effects vary. According to the Mach number values, we can classify the flow regimes in four classes, that are:

$*$*Subsonic regime* (for $\mathcal{M} < 1$), the flow velocity is lower than the speed of sound, shock waves do not appear in the flow and the compressibility can be ignored.

$*$ *Transonic regime* (for $\mathcal{M} \sim 1$), the flow velocity approaches the speed of sound, shock waves and compressibility effects begin to appear.

$*$*Supersonic regime* (for $1 < \mathcal{M} < 5$), the flow velocity is higher than the speed of sound. The study of shock waves be more important in this regime, they are generated by the collision between the object surface and fluid particles, and the compressibility effects are most important.

$*$*Hypersonic regime* (for $\mathcal{M} > 5$), the flow velocity is much higher than the speed of sound. As flow speed increases, the gas temperature increases, which results the ionization and dissociation of fluid molecules behind the shock waves.

1.4 Viscous forces

To study the real fluid flow we must take into account the effect of internal fraction (viscosity) and thermal conduction, that cause an irreversible transfer of thermodynamical properties and lead to dissipation of the energy during the fluid motion. Viscosity generates an irreversible transfer of momentum from regions where the velocity is large to those where it is small. Thermal conduction induces a thermal energy transfer from regions where the temperature is high to those where it is low, this transfer occurs because there is a heat transfer between the different parts of the system resulting from the nonuniform distribution of the fluid temperature throughout its volume.

If we apply some deformations to any real fluid, they realize an internal stress inside it. The total force acting on the whole volume of this continuous medium is given by the integral:

$$\int F_i dV \tag{1.16}$$

where F_i is the internal stress vector. We can write the vector F_i as a divergence of a tensor,

$$F_i = \frac{\partial \sigma_{ij}}{\partial x_j} \tag{1.17}$$

σ_{ij} is a symmetrical rank two tensor, called *the stress tensor*, which give the flux of the i component of the momentum in the j direction, takes the following form

[*Lan*87]

$$\sigma_{ij} = -p\delta_{ij} + \sigma'_{ij} \tag{1.18}$$

The first term represents the force exerted on the fluid element due to thermal pressure differentials. σ'_{ij} is *the viscous sterss tensor* which represents the irreversible transfer of momentum.

Such friction can occur in different fluid parts only when these parts have different velocities. If the gradients are small, we can suppose that σ'_{ij} depends only on the first derivatives of the velocity. Furthermore, we suppose that the dependence is linear. The most general explicit form of the viscous stress tensor is [*Lan*87],

$$\sigma'_{ij} = \eta \left\{ \frac{\partial v_i}{\partial x_j} + \frac{\partial v_j}{\partial x_i} - \frac{2}{3}\delta_{ij}\frac{\partial v_k}{\partial x_k} \right\} + \xi\delta_{ij}\frac{\partial v_k}{\partial x_k}$$

where $\eta\,[g.cm^{-1}.s^{-1}]$ is called *shear* or *dynamic viscosity*, represents the resistance of a fluid to flow. It can be expressed from the kinetic theory of gases, by

$$\eta = \frac{1}{3}\rho\lambda u \tag{1.19}$$

with λ is the mean free path of the particles and u is their random velocity relative to the mean flow. We also can define η by

$$\eta = \nu\ \rho \tag{1.20}$$

with $\nu\,[cm^2.s^{-1}]$ is the kinematic viscosity, given as

$$\nu = \frac{1}{3}\lambda u \tag{1.21}$$

ξ is called *second viscosity*, it can be given by [*Dur*08]

$$\xi = -\frac{2}{3}\eta \tag{1.22}$$

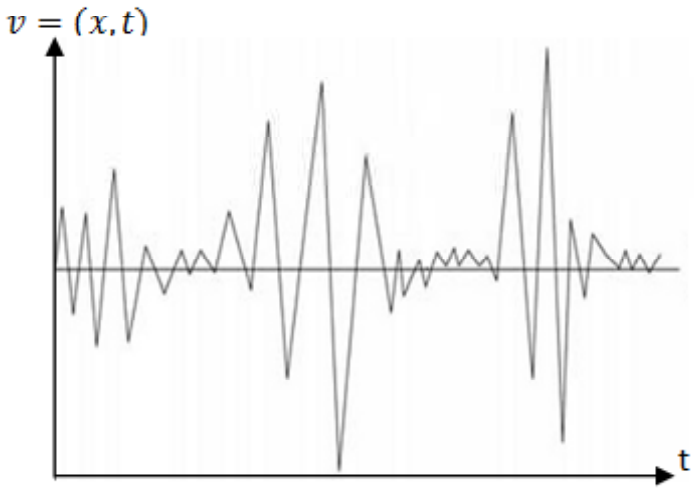

Figure 1.2: The velocity fluctuation at a point in turbulent flow.

This viscosity related with the internal degrees of freedom of molecules in the fluid. Therefore, ξ is zero for the perfect monoatomic gases.

1.5 Turbulence theory

Turbulence is a property of flows, not that of fluids. Therefore, the fluid flow can occur in two different types which are:

-*Laminar flow or streamline*; where the fluid moves in straight paths with an orderly and slowly motion. In this flow type, the viscous forces are dominant enough to keep all the fluid particles in parallel adjoining layers and move with constant properties (velocity, pressure,..) at each point as time passes.

-*Turbulent flow*; where the fluid flows faster and suffers irregular fluctuations, or mixing, and the flow properties (velocity, pressure,..) are rapidly and randomly varied in both magnitude and direction, from moment to moment (depends on the instant of observation). ($Fig\ 1-2$) represents the signal of velocity at a point in

Figure 1.3: Image of Orion Nebula show the turbulent environment of a stellar nursery consisting of stars in the earliest stages of formation, (Photo NASA/ESA).

turbulent flow, we note that the velocity component fluctuates around an average value known by the mean velocity.

In astrophysical and cosmological situations, the turbulence plays a crucial role by the interplay with other physical processes, like gravitation and magnetic field. The turbulent flow is the most common type in astrophysical problems such as the formation of the large scale structures in the universe that are the stars, where their formation takes place in highly dense turbulent molecular clouds ($Fig\ 1-3$), and the interaction between the interstellar turbulence and gravity is one of the most important reasons responsible for that stellar birth. Turbulence is also very important in the evolution of stellar structure, for which the turbulence carries the newly produced chemical elements from the centre to the outer layer of the star, this chemical change can influence the transport of mass, angular momentum and

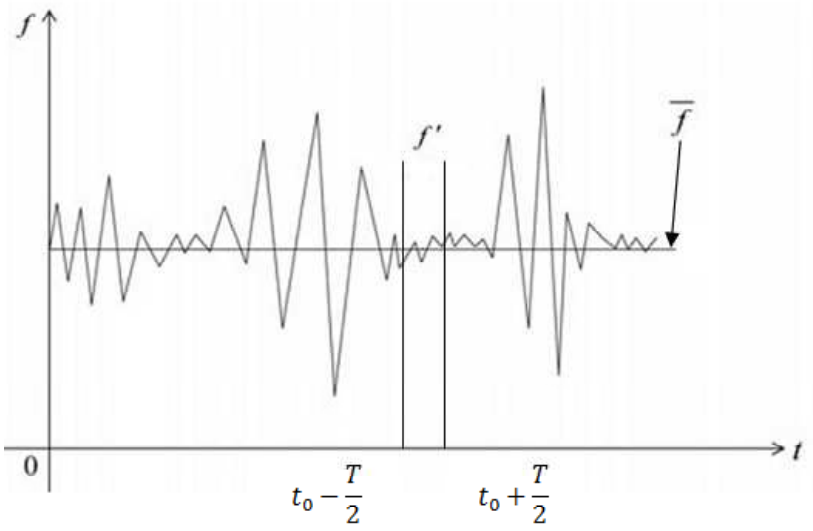

Figure 1.4: The mean and fluctuating values of a turbulent flow variable.

a further evolution of the stars. The turbulence phenomena are often observed in many other astronomical objects such as solar corona, accretion disks, generation of stellar winds and jets.

1.5.1 Dynamics of turbulence

Turbulent flow is strongly rotational, therefore it is characterized by the presence of a large number of superposed eddies with different sizes which are distributed randomly. So, we can distinguish tow types of eddies, large and small. One of the most successful theories in the description of turbulent flow is Kolmogorov Theorem, which is concerned with the characteristics of different eddies formed during this flow, as their size and energy. With this theory, the flow is regarded as homogeneous (all points in space have the same properties) and isotropic (the

properties of this flow have no preferred direction). The hypothesis of this theory is that the energy passes from large to small eddies (cascaded) and dissipates due to the viscosity of the fluid that is important only for small eddies, and the kinetic energy is transformed into heat.

Another important theorem gives the statistical description of turbulent flow, is Reynolds theory, that uses the statistical or averaged properties of the flow by the decomposition of each flow variable f in two values, the mean $\overline{f}$ and the fluctuating value $f^{'}$ as in $(Fig\ 1-4)$. By the application of this theory, we find a new set of fluid equations that are simpler to resolve the problem of turbulence theory.

1.6 Relativistic fluid dynamics

Relativistic fluid dynamics has a wide field of use in modelling the modern astrophysical problems, that failed to be treated by the classical theory, such as the topic of the collisions of heavy nuclei, the collapse of stellar cores during the supernovae and cosmology, and without forgetting its crucial role in modelling the jets emerging from the active galactic nuclei and the gamma ray burst sources. Here, we just provide an introduction about this theory and its importance.

This theory has a great importance because it includes various terms which are completely neglected in the classical case, it describes the motion of relativistic fluids, and as we said for classical fluid dynamics, the relativistic fluid theory also needs five dependent functions to describe this state, which refer to points in a four-dimensional continuum spacetime. This theory is based on the geometry of

the spacetime and described by the metric, which is denoted by $g_{\mu\nu} = g_{\nu\mu}$ (a symmetric tensor). In the relativity theory, the distance between two spacetime points along a given curve can be given as

$$ds^2 = g_{\mu\nu}\ dx^\mu\ dx^\nu \tag{1.23}$$

where $\mu, \nu = 0, 1, 2, 3$ and $x^0 = t(c = 1)$, $x^1 = x$, $x^2 = y$, $x^3 = z$. To determine the nature of this curve, we must first determine the value of the quantity $g_{\mu\nu}V^\mu V^\nu$, where V^μ is a contravariant vector $^{<<}$the tangent vector to the curve$^{>>}$. So, we can consider three types: if $g_{\mu\nu}V^\mu V^\nu < 0$, the curve is timelike, if $g_{\mu\nu}V^\mu V^\nu > 0$, the curve is spacelike and it is null if $g_{\mu\nu}V^\mu V^\nu = 0$. In relativistic fluids, the particles paths are described by a timelike curves.

1.6.1 Relativistic hydrodynamics equations

In relativistic fluids, the particles are still conserved and the equations that describe their evolution are given by five conservation laws, which are

$$\nabla_\mu\ j^\mu = 0 \tag{1.24}$$

This is *the conservation law of matter current density* j^μ, where $j^\mu = \rho u^\mu$, ρ is the rest mass density, u^μ the 4-velocity of the fluid and ∇_μ is the covariant derivative associated with the 4-dimensional spacetime metric, this in addition to four equations that we get from the *the conservation law of stress-energy*,

$$\nabla_\mu\ T^{\mu\nu} = 0 \tag{1.25}$$

where $T^{\mu\nu}$ is a symmetric tensor exists at each event in spacetime, it contains information about energy density, momentum density and stress. The stress-energy tensor defines viscous fluid as

$$T^{\mu\nu} = \rho\,(1+\varepsilon)\,u^{\mu}u^{\nu} + (P-\zeta\theta)\,h^{\mu\nu} - 2\eta\sigma^{\mu\nu} + q^{\mu}u^{\nu} + q^{\nu}u^{\mu} \tag{1.26}$$

with the scalar $\theta = \nabla_{\alpha}u^{\alpha}$, it describes the divergence of the fluid world lines, ε is the specific internal energy, P the isotropic pressure, q^{μ} is the energy flux vector, $h^{\mu\nu} = u^{\mu}u^{\nu} + g^{\mu\nu}$ is the spatial projection tensor and $\sigma^{\mu\nu}$ is the spatial shear tensor defined by

$$\sigma^{\mu\nu} = \frac{1}{2}\left(\nabla_{\gamma}u^{\mu}\ h^{\gamma\nu} + \nabla_{\gamma}u^{\nu}\ h^{\gamma\mu}\right) - \frac{1}{3}\theta\ h^{\mu\nu} \tag{1.27}$$

In perfect fluids, the stress-energy tensor given by

$$T^{\mu\nu} = \rho h u^{\mu}u^{\nu} + p g^{\mu\nu}$$

where $h = 1 + \varepsilon + \frac{P}{\rho}$, it is the specific enthalpy.

The previous conservation laws can be closed by Einstein equation,

$$G_{\mu\nu} = 8\pi T_{\mu\nu} \tag{1.28}$$

where $G_{\mu\nu}$ is the Einstein tensor associated with the stress-energy tensor and the spacetime metric, this equation is given with the use of geometrized units $G = c = 1$. This equation describes the dynamics of the gravitational field in general relativity where the left hand side represents the curvature of spacetime as determined by the metric and the right side represents the matter-energy content of spacetime.

1.6.2 Computational relativistic astrophysical hydrodynamics

The theoretical framework for studying the problems of relativistic astrophysical hydrodynamics is more complicated than the classical limit. Therefore, many problems encountered in relativistic astrophysics need computational methods. In the last 10 years, active researches in the subject of computational astrophysical fluid dynamics have been progressed and a number of powerful numerical codes have been developped for simulating the application of relativity theory in the astrophysical environment. the most popular codes in use in relativistic astrophysics are

*Pluto: Pluto code is a Godunov-type code, it is written in C programming language and suitable for different astrophysical applications; Newtonian, relativistic, MHD or relativistic MHD. In this code, the source terms include gravity, rotations and optically thin radiative losses. Pluto works on non-uniform grids and runs either on a single processor or on parallel architectures.

*ZEUS: ZEUS are several different numerical codes for astrophysical gas dynamics in two and three-dimensions, they adapt with UNIX operating system and perform 2D and 3D simulations. These codes began only as a hydrodynamical codes then they expanded to include a wide variety of problems such as MHD, relativistic hydrodynamics and radiation hydrodynamics. ZEUS can provide a good simulation results for accretion, disks especially in the transport of angular momentum and the magnetorotational instability (MRI) , but it is difficult to apply

them with our possibilities, because it requires a powerful computers.

*Athena: Athena is a grid-based code, it was developed primarily for magnetohydrodynamical simulations but it is also used in other different astrophysical applications (HD, relativistic). This code is allowed for cartesian or cylindrical coordinates and for static (fixed) mesh refinement, it is built mainly to study the interstellar medium, star formation and accretion flows.

CHAPTER 2

Accretion disks

Lately, there has been a renewed interest for the study of structure and evolution of accretion disks. This is partly because the most energetic sources in the universe must necessary be powered by accretion of matter onto a central body. Another reason for this interest is the gathering of observational data and numerical simulations both have shown that the accretion disk is an inescapable part in the life of most stars. These disks are formed around newly born stars, where they appear as a nurseries of planets, around supermassive black holes in the nuclei of galaxies, in stellar binary systems and in many other astronomical cases.

In this chapter, we firstly give interest to the basic aspects of these disks and their formation mechanisms. Secondly, we clarify where we can find them in various astrophysical objects. Then, we will try to summarize the mechanisms of angular momentum transport which is the basic idea of most accretion disks models. Next, we will describe the fundamental physics and equations that govern the structure of the accretion disks, and we will discuss the standard solution of Keplerian accretion disks with constant viscosity. Finally, we will review the basics of the standard model based on the Shakura and Sunyaev α-prescription for the turbulent viscosity.

Figure 2.1: A protostar in NGC 1333 surrounded by a giant cloud of dust and gaz. Credit: NASA/JPL-Caltech/R. Gutermuth (Harvard-Smithsonian Center for Astrophysic).

2.1 Prototype of accretion disks

Accretion disk is gas and dust rotating around a central celestial body, formed from inflowing or accreting matter. This latter is pulled into the accretion disk from the interstellar medium or other stars, and it cannot fall directly onto the gravitating object because it has a considerable angular momentum, that forces it into orbits around the central object. It becomes hot until its gravitational potential energy is converted into thermal energy. Once in the disk, the matter loses its angular momentum and it slowly becomes spirals inward to fall onto the central body.

The accreting matter radiates energy away as infrared , visible, ultraviolet, and X-ray light, which astronomers detect and use to study both the accretion disk

and the central body. Accretion disk has a remarkable efficiency for converting gravitational energy into radiation or thermal energy. In the case of neutron stars, the conversion efficiency can exceed 10% of the equivalent rest mass energy of the accreting matter while the maximum efficiency can be achieved by rotating black holes; up to 30%.

2.2 Accretion process in astrophysics

2.2.1 Accretion process

In astrophysics, accretion means the infall of matter onto a celestial body due to the gravitational attraction of this body. The accretion process is the most effective way of extracting energy from a normal matter, this process is more efficient source of energy than nuclear fusion.

If a particle of mass dm falls from infinity and accretes onto an accretion disk in a circular orbit of radiu R around a star of mass M, from the centrifugal equilibrium we get

$$\frac{v^2 dm}{R} = \frac{GMdm}{R^2} \tag{2.1}$$

So, the accretion energy released by the particle is

$$dE_{acc} = dE_{\infty} - dE_R = \frac{GMdm}{R} \tag{2.2}$$

The accretion luminosity is the mass accreted per time interval dt

$$L_{acc} = \frac{dE_{acc}}{dt} = \frac{GM}{R}\frac{dm}{dt} \tag{2.3}$$

As long as this luminosity results from accretion, we can write

$$L_{acc} = \frac{GM\ \dot{M}}{R} \tag{2.4}$$

where $\dot{M}$ $[g.s^{-1}]$ is the accretion rate.

2.2.2 Spherical accretion

Spherical or Bondi accretion is the simplest type of accretion flow for treating because thermal pressure is the only force counteracting with gravity. In this case, the star placed in a static and uniform gaseous medium accreting a mass from its surroundings, and the angular momentum of the gas is negligible.

In general, accretion is not spherical as the disk is flattered by radiation, for that an outward transport of angular momentum can occur.

2.2.3 Eddington luminosity and the accretion rate

The Eddington luminosity or Eddington limit is the maximum luminosity that an object can emit without destroying itself, but there are other objects that can exceed this limit, like gamma ray bursts, novae and supernovae. At this limit, the outward force caused by radiation pressure is equal to the gravitation force, this latter pulles the gas inward. But if the luminosity of a star exceeds the Eddington luminosity, the radiation pressure overcomes the gravitational attraction and pushes away the infalling matter from the accretion disk that stops the accretion process, the star ejects its outer envelope like an intense stellar wind and it becomes instable .

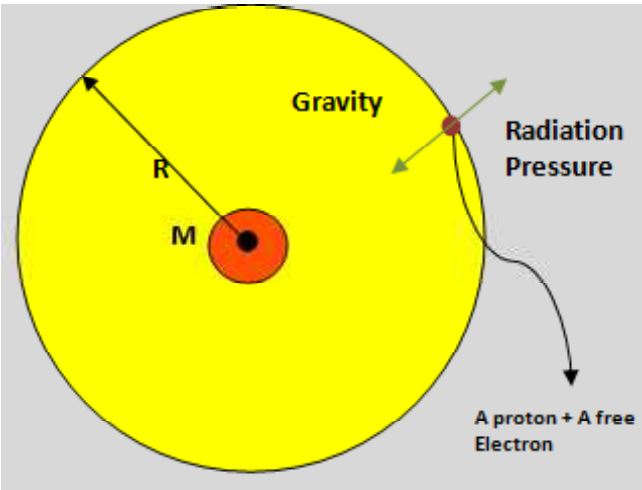

Figure 2.2: Scheme shows the Eddington limit.

To calculate this limit, we consider a volume of a fully ionized hydrogen with a steady spherical accretion, i.e, matter falling radially and uniformly onto the volume, the gravitational force is

$$F_g = \frac{GMm_p}{R^2} \tag{2.5}$$

And the force caused by radiation pressure is given by

$$F_r = \frac{L\sigma_T}{4\pi R^2 c} \tag{2.6}$$

Where L is the luminosity of the volume and σ_T is the Thomson scattering cross-section.

By equating these two forces, we find [$Fra02$]

$$L_{edd} = \frac{4\pi GMm_p c}{\sigma_T} \backsimeq 1.3 \times 10^{38} \left(\frac{M}{M_\odot}\right) erg.s^{-1} \tag{2.7}$$

We may also write

$$L_{edd} = \frac{GM\ \dot{M_E}}{R_0} \tag{2.8}$$

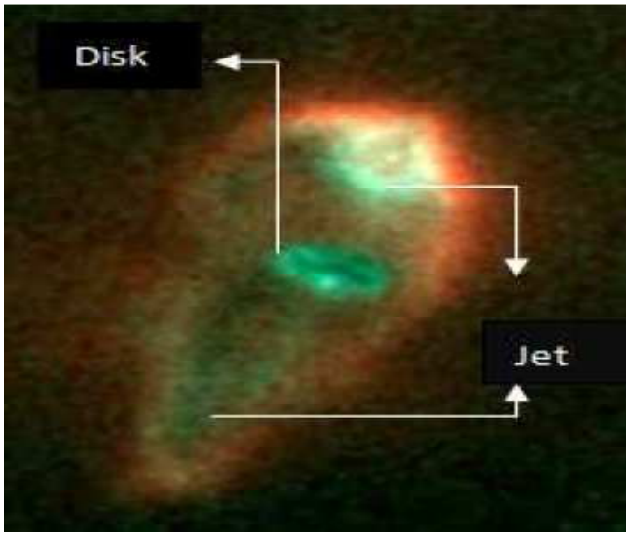

Figure 2.3: A protostar survives in Orion. Credit: J. Bally (U. Colorado), H. Throop (SwRI), C.R. O'Dell (Vanderbilt U.), NASA.

Where $\dot{M}_E$is the Eddington accretion rate, defined by [$Bal96$]

$$\dot{M}_E = 4\pi r_0 \frac{m_p c}{\sigma_T} \backsimeq \dot{} 9.5 \times 10^{11} R_0 g s^{-1} \tag{2.9}$$

r_0 is the innermost radius. $\dot{M}_E$ does not mean the maximum, because there exists no maximum on the accretion rate.

2.3 Disks in the universe

2.3.1 Protostellar and protoplanetary disks

The accretion process is an essential stage in the earliest formation of a star as at this phase of its life, it acquires most of its mass by accretion from the interstellar medium, where the disk is called *protostellar disk*. The star begins its life as a protostar whith a mass less than $10^{-2} M_\odot$ and it continues to grow while

the matter continues to fall onto it as accretion shocks on its surface. The initial stages of stars formation have been reviewed in various recent studies and we will only mention the stage where the accretion process is important [$Har96$].

A star formation starts with a gravitational collapse of an instable and dense mass within the molecular cloud, this mass may fragment into smaller cores to form a rotating prostellar cores. Once the core becomes optically thick and it is in hydrostatic equilibrium, the object now is called a protostar. The protostar is embedded in an extended optically thick envelope, whose gas rains onto the core with supersonic velocities. Under the effect of the magnetic field and the rotation, the envelope disperses and reveals the accretion disk, then the central star begins to bright and the spectrum components are seen in both visible and infrared .

Advances in telescope technology has revealed some unexpected characteristics of both disks and young stars that were not predicted by any theoritical models . ($Fig\ 2-3$) shows that the protostar drives an energetic bipolar jet into its surroundings, they have already appeared very early during the 10^4 years of evolution when the protostar was still obscured. The energy source of this outflow is believed to be caused by the coupling of the helical magnetic field with the inner parts of the circumstellar disk or with the central protostar.

Accretion disks not only play an important role in star formation, but in planet formation as well. The protoplanetary disks are equally supposed to be the planets formation place. In 1995, Mayor and Queloz have discovered the first extrasolar planet. Since then, more than 400 planets have been discovered around near stars

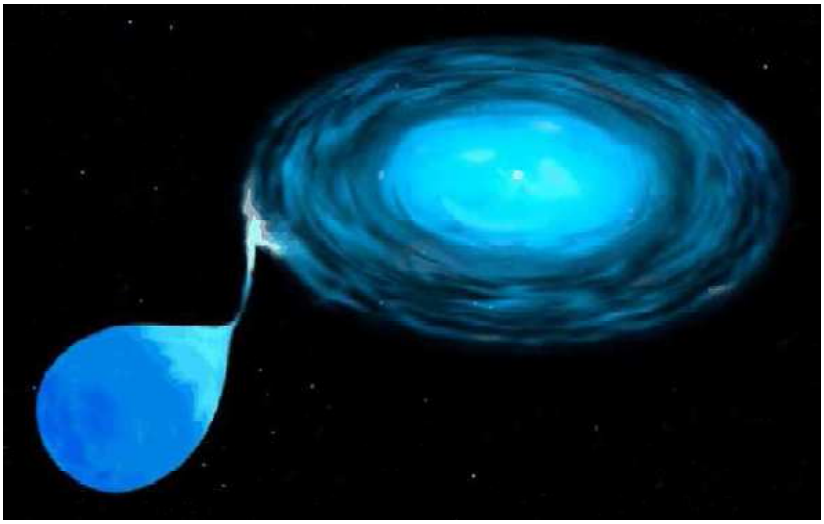

Figure 2.4: Artist's conception of binary system with giant star and compact object. Crédit: Nasa/Space Telescope Science Institute.

similar to the sun.

The planets are formed where the disk is dense enough, the dust grains lean to be placed on one another, bonded by ices and eventually form the rocky cores of planets. To form a gaseous giant planet such as jupiter, the core must subsequently capture and accrete gas from the nearby disk.

2.3.2 Close binary systems

Observations show that the great majority of stars are formed in binary or multiple systems. The formation of these systems is the usual result of a rotating cloud core fragments during the isothermal phase of collapse [$Clar01$]. If the binary system contains a sufficient massive star ($M \succ 2M_{\odot}$) [$Sha73$] and another star may still be on the main sequence of stellar evolution, the primary star loses its

stability and collapses to reach the end of its life as a compact object; *white dwarf* , *neutron star* or *black hole*. When this happens, the strong gravitational field of the compact object leads the normal star to overflow its critical equipotential surface or Roche lobe and its matter falls onto the compact star [$Fra02$].

When the stars are close enough to each other, centrifugal forces become comparable to gravitational forces, the accreting matter begins to rotate in circular orbits to form an accretion disk around the compact object, it gradually loses its angular momentum by several mechanisms to spiral inward and fall onto the compact object. We distinguish two types of interacting binary stars and they are:

Cataclysmic variables (CV)

Cataclysmic variables are a close binary systems containing a primary white dwarf and a secondary main sequence or a red giant star. This type is characterized with an accreting mass flowing from the secondary towards the primary and forms an accretion disk around the white dwarf. The orbital period of these binaries generaly varies from 80 min to 15 h. The destiny of the white dwarf depends on the accretion rate $\dot{M}$:

$*$ if $\dot{M} \approx (10^{-11} - 10^{-8})\, M_{\odot} yr^{-1}$, the accreting gas accumulates on the surface of the white dwarf where it is compressed and heated. At the surface accumulated hydrogen layer, density and temperature rise enough so that, thermonuclear interaction occurs, and it rapidly burns the hydrogen layers into helium causing the eruption of novae.

$*$ if $\dot{M} \approx (10^{-8} - 10^{-6})\, M_{\odot} yr^{-1}$, the accretion process continues and the star mass closes to the Chandrasekhar mass ($1.4 M_{\odot}$), carbon burning begins at the center of the star in the degenerate core and moves towards the surface. This subsonic motion converting approximately one half of the white dwarf mass into Iron, completely disrupts the star causing it to explode in the form of a supernova type Ia.

$*$ Up to 10^{-6}, we can not observe the debris of the explosion because the white dwarf is embedded in a large envelope.

X-ray binaries (XRB)

X-ray binaries are a close binary systems containing a primary neutron star or a black hole and a secondary main sequence or a red giant star. The matter transfers from the secondary to the primary star and forms an accretion disk around it. The accreting matter becomes very hot and liberates gravitational potential energy up to several tenths of its rest mass as X-rays.

XRB's are the brightest X-ray sources in our galaxy and they are characterized with dramatic variabilities in brightness on timescales ranging from milliseconds to months and years; hydrogen accumulates on the surface of the primary star, density and temperature increase and when they are high enough, explosions on the primary star surface happen. There are two types of X-ray binaries, and the mass of the companion star (secondary) determines the type of accretion that occurs [$Clar01$].

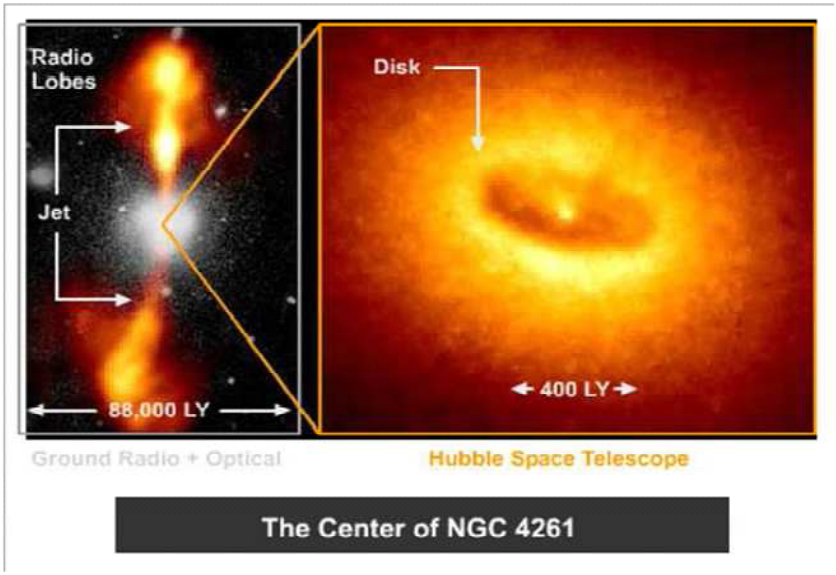

Figure 2.5: Hubble space telescope image shows the core of an AGN, NGC 4261.

∗ Law-mass X-ray binaries (LMXB): Involving a secondary star with a mass smaller than or comparable to that of the sun, the accretion occurs through roche lobe overflow.

∗ High-mass X-ray binaries (HMXB): These binaries are strong in X-rays in which the secondary is a massive star ($M \geqslant 10M_{\odot}$). The secondary of high mass pushes its matter on the shape of a wind in the space, so a portion of it runs into the primary star to start the accretion process around it.

2.3.3 Active galactic nucleus (AGN)

It is wide accepted now that the center of most or all galaxies hosts a super-massive black hole (of up to some millions solar masses). The huge mass of these objects grows, which means that galaxies are active from time to time. AGN's

are the brightest objects in the universe, which are prominent across the whole electromagnetic spectrum and they often have a peak from radio to gamma-ray .

In addition to their large variability in the continum and spectral line emission, they have enormous powerful outputs many billions of times the luminosity of our sun (up to $10^{49} erg/s$). But as we know that the black hole emits nothing, so the radiation from an AGN is believed to come from material heated to several million degrees, this material close to the central black hole forms an accretion disk before it falls into the black hole .

The modern observational technology has observed the existence of another structure similar to the accretion disk, it is a torus of matter formed around the disk, containing gas, dust and a debris of disrupted stars due to the close passage from the black hole [$Har06$]. Radio observations of AGN's often show powerful jets which are extended linear beams that transport energy and particles from the compact source to the extended regions.

2.3.4 Other astrophysical disks

In addition to the previously mentioned, there are many other examples of accretion disks in universe.

Compact binaries

Compact binaries are a close massive binary systems, containing two compact stellar remnants (a white dwarf, a neutron star or a black hole). Because the grav-

Figure 2.6: Images of Black hole devours neutron star. Credit: Dana Berry/NASA.

itational field of the compact objects is so intense, the stars lose their energy while emitting gravitational waves and spiral closer and closer together with velocities converging the speed of light. When they sufficiently approach, tidal forces strip the less massive companion to form an accretion disk around the more massive.

In some cases (double neutron stars binaries, black hole and white dwarf binaries or black hole and neutron star binaries), the stars quickly merge (have been proposed for the first time by Paczynski in 1986) and form a single black hole with a torus of torn debris which is the accretion disk, where the matter rapidly accretes onto the central black hole and produces a twin of relativistic jets out along the rotation axis, $(Fig\ 2-6)$.

Each formation of a black hole by the coalescence of two compact objects liberates a huge energy ($\backsim 10^{53} erg.s$) in the form of fireballs of a short duration gamma-ray bursts(<2sec).

Herbig Ae/Be stars (HAEBE)

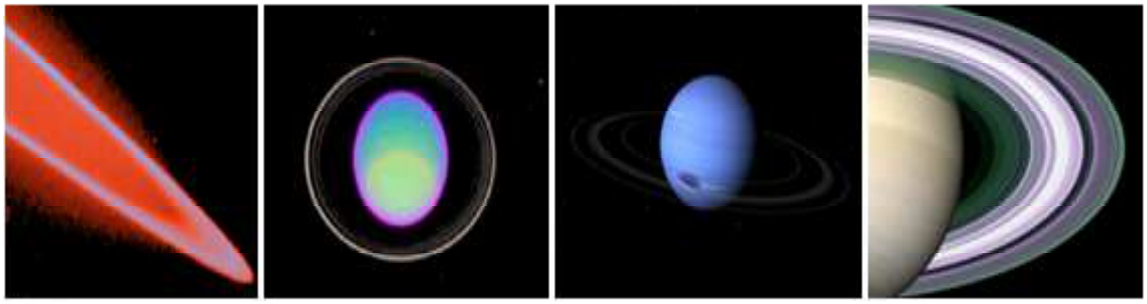

Figure 2.7: Images show from left to right the rings of Jupiter, Uranus, Neptune and Saturn.

HAEBE's are pre-main sequence stars with mass of 2 to 10 solar masses and strong hydrogen and calcium emission lines. They are fast rotators, hotter and brighter than lower mass stars T Tauri (stars with $M < 2M_{\odot}$) and live shorter because they spend less time contracting toward the main sequence. These young stellar objects are embedded in a massive molecular cloud of gas and dust, perhaps arranged in a circumstellar accretion disk which associated with strong outflow of infrared excess radiation due to free-free emission.

Planetary rings

Planetary rings are very thin rings surrounding the planets, they share some dynamical properties with gaseous accretion disks. They compose of ice particles ranging in size from dust to boulders of few meters in diameter. These ring systems are present at all gas giant planets of our solar system, they exist around Jupiter, Uranus, Neptune and Saturn, which is the only whose rings are easily visible through telescopes. The origin of these ring systems is still controversial.

Spiral galaxies

Since more than half of the observed galaxies are spiral, spiral galaxies are the most common type in the univers, they be in the form of rotating disks of gas, dust and stars. This galaxies have a complex structures with three components: spiral arms, bulge, and halo. The spiral arms are regions of active star formation, they are rich in gas, dust and youngest stars as blue and blue-white which make the spiral arms extremely visible. The bulge is the nucleus of the galaxy, it is much more dense and red in color due to the presence of many old stars in this region as red stars, and at the very center, can be found a supermassive black hole containing millions of times the mass of the Sun. Spiral galaxies are embedded in an invisible and large halo of gravitating material which consists of stars, dark matter and globular clusters of stars.

Disks of spiral galaxies are not Keplerian, they are strongly self gravitating and the accretion processes need a long time-scales more than in stars.

Our galaxy, Milky Way, and the nearby Andromeda Galaxy, are both large spiral galaxies. The image below left shows a nice spiral galaxy, NGC 3810, and the right image shows Milky Way galaxy in a position allows to illustrate the components of spiral galaxies.

Figure 2.8: First image: NGC 3810 galaxy. Second image: Milky Way galaxy. Credit: ESA/Hubble and NASA.

2.4 The transport of angular momentum in accretion disks

To understand the structure, stability and evolution of accretion disks, we must understand the mechanisms which are responsible for the outward transport of angular momentum in them. As mentioned previously, the disk matter cannot fall directly, but it remains rotating around the central object because it has enough angular momentum. Accretion of gas toward the central object requires physical processes that can extract angular momentum of the rotating matter to break the equilibrium between gravity and centrifugal force.

Naturally, the fluid viscosity could play this role. However, the calculations of the molecular viscosity by Spitzer in 1962 show that it is too small to be important. Other calculations show that the hydrodynamic viscosity is able to replace the effect of molecular viscosity [$Lyn74$]. The first model which assumed the effect

of turbulent viscosity in the transport of angular momentum is the phenomenological "alpha-viscosity prescription", introduced by Shakura and Sunyaev [$Sha73$] as known as *the standard model*, it gives a good estimate to the order of the viscosity magnitude but the problem here is the unknown source of viscosity, because the disk is expected to be turbulent, so it has a high Reynolds number, i.e, a low molecular viscosity.

The outward transport of angular momentum can occur if the disk is subject to internal torques (can either be gravitational or turbulent) or external torques (can either be magnetic or tidal) [$Pap95$], [$Bal03$].

2.4.1 Magnetohydrodynamical turbulence

In the magnetized disks, when the degree of ionization is sufficient and magnetic coupling with gas is important, the magnetorotational instability MRI can be much more effective to initiate and sustain magnetohydrodynamical turbulence MHD. This latter is one of the most important ways of removing angular momentum. MRI has been studied following the researchs of Balbus and Hawley [$Bal96$], and since 1995 it has been considered as a possible source of transport in accretion disks. if a disk obeys to the MRI, the only criterion for this instability is $(d\Omega^2/dr) < 0$, that the angular velocity Ω of the disk decreases outwards. The MRI is limited only if the magnetic field exceeds a certain strength or if the gas is insufficiently ionized, this means that it may be neglected in large protoplanetary disks.

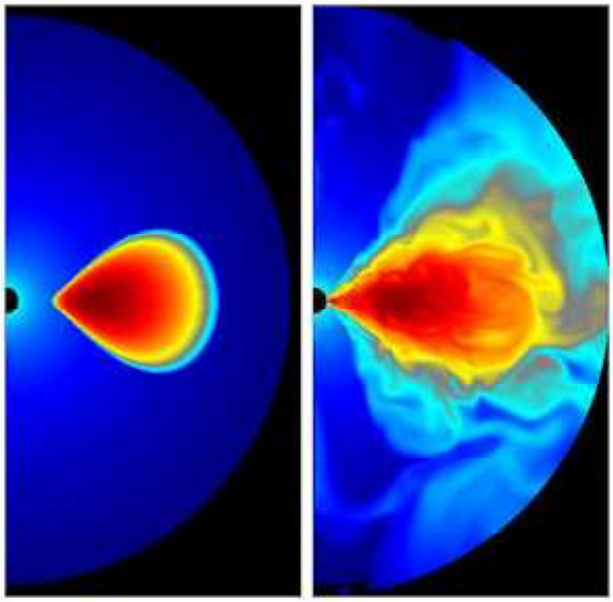

Figure 2.9: Numerical simulation by [Haw97], shows the developement of the MRI in an accretion disk.

This transport mechanism appear naturally in disks that reside around compact objects, where the accretion flow is hot and the ionization level is sufficient, but this is not realized for the protoplanetary disks where the accretion flow is cold. Actually, many researches have proved that this kind of instability is more effective in both outermost and innermost parts where the first is sufficiently ionized by cosmic rays and the second by radiation from the central object, thus leading to develop a ≪dead zones≫ in the disk.

2.4.2 Self-gravitating transport

The transport with self-gravitating instability is another important mechanism. If the disk mass is sufficiently large compared to that of the star, gravita-

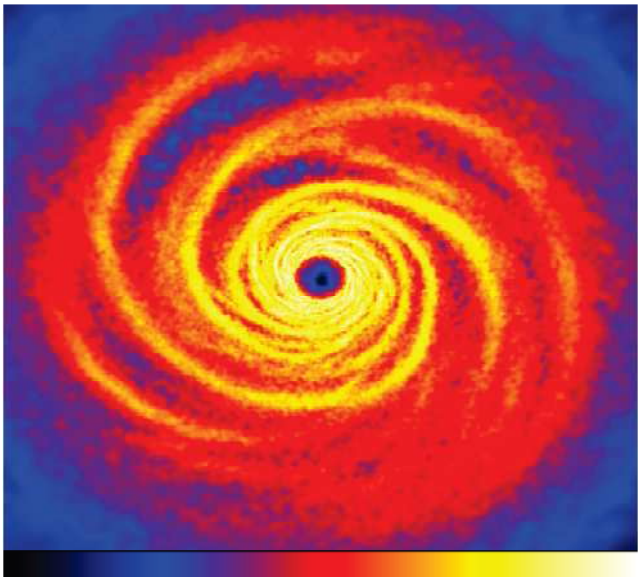

Figure 2.10: Surface density structure of a self-gravitating disk. From [*Ric*06].

tional instabilities become important. Weak gravitational instability may generate spiral density disturbances (the form of spirals is the result of differential rotation) [*Pap*95], which are responsible for removing the disk matter inward and the angular momentum outward. $(Fig2-10)$ is a snapshot taken from an hydrodynamical simulation of self-gravitating disks, it shows the spiral structure. The criterion governing the importance of disk self-gravity is *the Toomre criterion*,

$$Q \simeq \frac{c_s k}{\pi G \Sigma} \tag{2.10}$$

where Σ being the mass density, k being the epicyclic frequency in the disk, defined by the relation

$$k^2 = \frac{1}{r^3}\frac{d(R^4\Omega^2)}{dr} \tag{2.11}$$

Q is a dimensionless parameter, its role is to determine whether a gaseous disk is gravitationally unstable or not, hence

*if $Q < 1$, Instability in cylindrical symmetry develops in the disk.

*if $Q > 1$, The disk is stable (this is the case of disks with low mass).

*if $Q \simeq 1$, Asymmetric instabilities appear in the disk .

this mechanism proceeds only in very massive disks such as those formed in the earliest stages of stars formation where the disk mass is more than that of the protostar. Over time, this instability becomes negligible because the quick redistribution of disk matter leads to reduce its mass by the accretion onto the central star.

2.4.3 Tidal torque

If two stars of binary system are adequately close, the orbiting companion exerts a tidal torque to the outer layers of the disk, which leads to an outward exchange of angular momentum from the disk rotation to the orbital motion of the binary. Such tidally torques create spiral disturbances in the accretion disk, which propagate inward as acoustic waves carry negative angular momentum [$Liv91$]. The effect of tidal waves does not only exist in interacting binary stars, but it can be generated by objects that are formed in the disk itself, like massive planets, satellites and the impact of Saturn's moons on its rings. A tidal torque is proportional to the object mass, whenever the object mass increases, its gravitational attraction and its impact on the disk increase.

We finally notice, that all these mechanisms which are described above, can interact in very complicated ways and play an essential role in the transport of

angular momentum in accretion disks .

2.5 The basic equations of accretion disks

In this section we set up the basic equations that govern the structure of accretion disks.

*Conservation laws

Since the basic idea of most accretion disks models is to study the outward angular momentum transport and the inward mass transport in it, the evolution of an accretion disk is organized by two conservation laws; conservation of mass and conservation of angular momentum. In this thesis, we adopt the assumption that the disk is axisymmetric, i.e. $\frac{\partial}{\partial\phi} = 0$ or that no quantity depends on the azimuthal angle ϕ, and the z-axis is the axis of rotation and that both conservation laws are in cylindrical polar coordinates (r, ϕ, z) centred on the star. So,

The continuity equation is

$$\frac{\partial\rho}{\partial t} + \frac{1}{r}\frac{\partial\left(\rho r v_r\right)}{\partial r} + \frac{\partial(\rho v_z)}{\partial z} = 0 \tag{2.12}$$

The Navier-Stokes equations with ($\rho =$ costant) and g_{eff} is the effective gravity, [$Spu08$] is

$$\begin{aligned} r \quad : \quad & \rho\left\{\frac{\partial v_r}{\partial t} + v_r\frac{\partial v_r}{\partial r} + v_z\frac{\partial v_r}{\partial z} - \frac{v_\phi^2}{r}\right\} = -\frac{\partial P}{\partial r} + \rho g_{eff_r} + \frac{\partial}{\partial r}\left(\eta\frac{\partial v_r}{\partial r}\right) \\ & + \frac{\partial}{\partial z}\left(\eta\frac{\partial v_r}{\partial z}\right) + \frac{1}{r}\frac{\partial}{\partial r}\left(\eta v_r\right) - \eta\frac{v_r}{r^2} \end{aligned} \tag{2.13}$$

$$\begin{aligned} \phi \quad : \quad & \rho\left\{\frac{\partial v_\phi}{\partial t} + v_r\frac{\partial v_\phi}{\partial r} + v_z\frac{\partial v_\phi}{\partial z} + \frac{v_r v_\phi}{r}\right\} = \rho g_{eff_\phi} + \frac{\partial}{\partial r}\left(\eta\frac{\partial v_\phi}{\partial r}\right) \\ & + \frac{\partial}{\partial z}\left(\eta\frac{\partial v_\phi}{\partial z}\right) + \frac{1}{r}\frac{\partial}{\partial r}\left(\eta v_\phi\right) - \eta\frac{v_\phi}{r^2} \end{aligned} \tag{2.14}$$

$$z \quad : \quad \rho\left\{\frac{\partial v_z}{\partial t}+v_r\frac{\partial v_z}{\partial r}+v_z\frac{\partial v_z}{\partial z}\right\}=-\frac{\partial P}{\partial z}+\rho g_{eff_z}+\frac{\partial}{\partial r}\left(\eta\frac{\partial v_z}{\partial r}\right)$$
$$+\frac{\partial}{\partial z}\left(\eta\frac{\partial v_z}{\partial z}\right)+\frac{1}{r}\frac{\partial}{\partial r}\left(\eta v_z\right) \tag{2.15}$$

If the disk is geometrically thin, we use only the ϕ-component of Navier-Stokes equations, because the circular velocity v_ϕ is the dominant with a small radial velocity $v_r\left(r,t\right)$ [$Cla07$]. In this case the matter moves very close to the plane $z=0$ (where, $z=0$ is the mid-plane of the disk), i.e. $v_z=0$. However, in the case of geometrically thick accretion disks, the calculation become more complicated because we need to use the three components of the Navier-Stokes equations.

*Angular velocity

The angular velocity $\Omega\left(r\right)$ is

$$\Omega\left(r\right)=\frac{v_\phi}{r} \tag{2.16}$$

But when the disk is Keplerian, the angular velocity becomes $\Omega\left(r\right)=\Omega_K\left(r\right)$. For this approximation, the matter moves with a centrifugal force balanced with the gravitational force, so

$$\Omega_K^2\ r=\frac{GM}{r^2} \tag{2.17}$$

thus

$$\Omega_K=\left(\frac{GM}{r^3}\right)^{\frac{1}{2}} \tag{2.18}$$

where M is the mass of the accreting star and $G=6.674\times10^{-8}cm^3g^{-1}s^{-2}$ is the gravitation constant.

*Surface density

To get the expression of the surface density we integrate the density ρ in the vertical direction [$Cla07$], so

$$\Sigma = \int \rho dz = \rho H \tag{2.19}$$

with $\Sigma\,[g.cm^{-2}]$ is the mass per unit surface area of the disk.

*Disk thickness

We take the typical thickness of the disk in the z-direction H. Where for geometrically thin disks is small compared to its radius; $H \ll R$, and for geometrically thick disks $H \backsim R$. In thin-disk approximation, H is defined by [$Fra02$]

$$H \cong c_s \left(\frac{r}{GM}\right)^{1/2} r \cong \frac{c_s}{\Omega} \tag{2.20}$$

c_s is the sound speed, it is given in relation of the total pressure of the disk

$$c_s^2 = \frac{P}{\rho} \tag{2.21}$$

The thin-disk approximation requires that the disc flow is highly supersonic because the sound speed c_s is much less than the rotational velocity $r\Omega\,(r)$.

*Viscous torque

The viscous torque is the flux of angular momentum transported by viscosity across an annulus of the disc. We consider that the disk takes the form of adjacent annuli. Such annulus limited between inner radius r and outer radius $r + \Delta r$, ($Fig\ 2-11$), its mass is $2\pi r\Sigma.\Delta r$ and its angular momentum is $2\pi r\Sigma.\Delta r.r^2\Omega$. $G\,(r,t)$ is the viscous torque of an outer annulus acting on a neighboring inner one

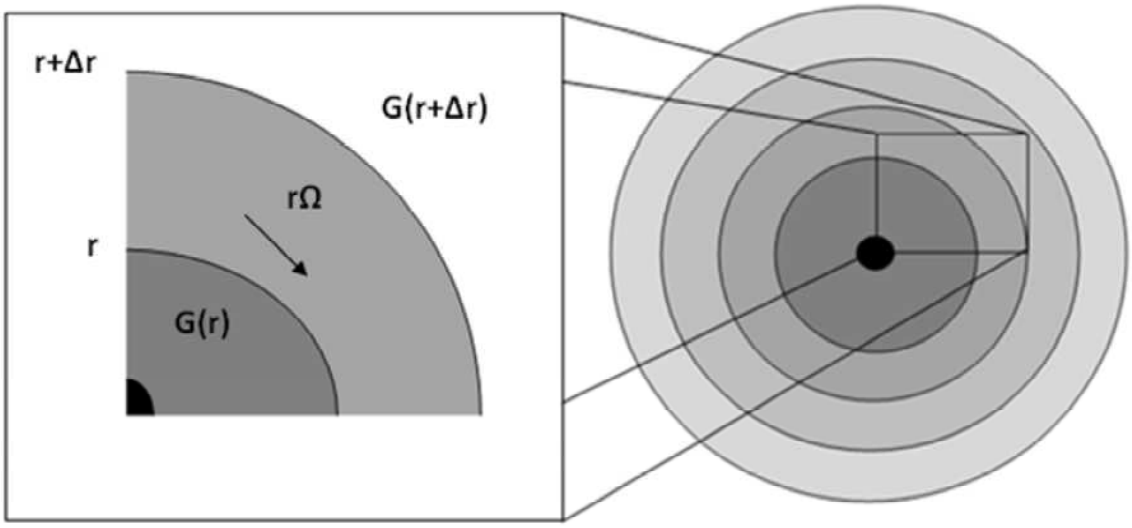

Figure 2.11: Schematic view shows the disk rings and the differential viscous torque.

at radius r, thus [$Pri81$]

$$G\left(r,t\right)=2\pi r.\nu\Sigma A.r \tag{2.22}$$

where A is the rate of shearing defined by

$$A=r\frac{d\Omega}{dr} \tag{2.23}$$

So, equation (2.22) becomes

$$G\left(r,t\right)=2\pi\nu\Sigma r^{3}\frac{d\Omega}{dr} \tag{2.24}$$

It is very important to take into account this fluid property because it is one of the fundamental agents responsible for the redistribution of angular momentum, that leads to spread the annuli and to transport the matter toward the smaller radii to be accreted dy the central star.

Disk pressure

Since we are interested with fully ionized disks, the total pressure P is the sum of the two quantities; gas pressure due to particles and radiation pressure due to photons, hence

$$P = \frac{\rho K T}{\mu m_p} + \frac{4\sigma}{3c} T^4 \tag{2.25}$$

where

$$P_{gas} = \frac{\rho K T}{\mu m_p} \quad \text{and} \quad P_{rad} = \frac{4\sigma}{3c} T^4 \tag{2.26}$$

K is Boltzmann's constant, σ the Stefan Boltzmann constant, and μ the mean molecular weight, for fully ionized cosmic matter $\mu \simeq 0.615$. The gas pressure can dominate over the radiation pressure except in some cases as the innermost part of luminous disks around black holes.

*Optical depth

The optical depth τ represents the number of interactions suffered by a photon between the equatorial plane and the surface of the disk where will be liberated, thus

$$\tau = \rho \; H \; \kappa_R \left(\rho, T\right) = \Sigma \; \kappa_R \left(\rho, T\right) \tag{2.27}$$

with $\kappa_R \left(\rho, T\right)$ is *the Rosseland mean opacity.* This relation is verified for optically thick and thin disks, where if $\tau \lesssim 1$, the disk is called optically thin, in this case the photon can escape directly from the gas without a further absorption or reemission, this a property of stellar atmosphere. While if $\tau \gg 1$, the disk is called optically thick, this is a property of stellar interiors.

*Rosseland mean opacity

The Rosseland mean opacity is the most widely used opacity in the study of disks with high-temperature. The opacity determines the interaction between matter and radiation, it is generally depends on the chemical composition of the gas, density and temperature. Therefore, it should have the following form

$$\kappa = \kappa\left(\rho, T, chemical\ composition\right) \tag{2.28}$$

Several calculations have been done to define the opacity formula, the OPAL opacity project at Lawrence Livermore National Laboratory approximate a power-law form which is more appropriate for use to solve the equations of disk structure, is

$$\kappa = \kappa_0\ \rho^a\ T^b \tag{2.29}$$

where a, b, and κ_0 are constants depend on the regimes of opacity. For accretion disk around a compact star, the opacity is given by two values:

First, *Thomson opacity,* it represents the scattering of photons by free electrons and holds when the temperature of the disk is $T > 10^4 K$ $[Fra02]$

$$\kappa = \text{constant} \simeq 0.34\ cm^2 g^{-1} \tag{2.30}$$

Second, *Kramer opacity*, it holds when free-free and bound-free transitions are dominant and the temperature of the disk is below $10^4 K$, $T \lesssim 10^4 K$ $[Fra02]$.

$$\kappa = 4.5 \times 10^{24} \rho\ T^{-7/2}\ cm^2 g^{-1} \tag{2.31}$$

Energy transport equation <<the temperature equation>>

The temperature of an accretion disk is given by the relation [$Fra02$]

$$\frac{4\sigma}{3\tau}T^4 = D(r) \tag{2.32}$$

with $D(r)$ is *the viscous dissipation rate* per unit face area, represents the energy flux through the faces of the disk due to the viscous torques G, so

$$D(r) = \frac{G}{4\pi r}\frac{d\Omega}{dr} \tag{2.33}$$

$4\pi r$ is the plane area of each ring, with the viscous torque in relation (2.24), we get

$$D\left(r\right) = \frac{1}{2}\nu\Sigma r^2\left(\frac{d\Omega}{dr}\right)^2 \tag{2.34}$$

We consider as a particular case, the Keplerian case, so $D\left(r\right)$ becomes

$$D\left(r\right) = \frac{9}{8}\nu\Sigma\ \frac{GM}{r^3} \tag{2.35}$$

and the energy transport equation is

$$\frac{4\sigma}{3\tau}T^4 = \frac{9}{8}\nu\Sigma\ \frac{GM}{r^3} \tag{2.36}$$

2.6 Keplerian accretion disks

We start by the study of thin Keplerian accretion disks, because it helps us to understand the effect of viscosity on the outward transport of angular momentum, which can be then generalised to thick disks. As we mentioned earlier that the evolution of an accretion disk is described by the two laws of conservation (1.1) and (1.5) in cylindrical polar coordinates (r, ϕ, z). In the following study, we regard

the disk as geometrically thin, stationary and Keplerian, so the continuity equation (2.12) becomes

$$\frac{\partial \rho}{\partial t} + \frac{1}{r}\frac{\partial \left(\rho r v_r\right)}{\partial r} = 0 \tag{2.37}$$

and the ϕ-component of Navier-Stokes equations (2.14) becomes

$$\rho\left\{\frac{\partial v_\phi}{\partial t} + v_r\frac{\partial v_\phi}{\partial r} + \frac{v_r v_\phi}{r}\right\} = \frac{\partial}{\partial r}\left(\eta\frac{\partial v_\phi}{\partial r}\right) + \frac{\partial}{\partial z}\left(\eta\frac{\partial v_\phi}{\partial z}\right) + \frac{1}{r}\frac{\partial}{\partial r}\left(\eta v_\phi\right) - \eta\frac{v_\phi}{r^2} \tag{2.38}$$

where the pressure and gravitational forces do not give any contribution due to the assumption of axisymmetry. Now, we include the surface density Σ in the above equations by integrating in the vertical z-direction. The introduction of Σ will help us to eliminate any z term, so equations (2.37) and (2.38) become respectively

$$\frac{\partial \Sigma}{\partial t} + \frac{1}{r}\frac{\partial}{\partial r}\left(r\Sigma v_r\right) = 0 \tag{2.39}$$

and

$$\Sigma\left(\frac{\partial v_\phi}{\partial t} + v_r\frac{\partial v_\phi}{\partial r} + \frac{v_r v_\phi}{r}\right) = \frac{\partial}{\partial r}\left(\Sigma\nu\frac{\partial v_\phi}{\partial r}\right) + \frac{1}{r}\frac{\partial}{\partial r}\left(\Sigma\nu v_\phi\right) - \frac{\Sigma\nu\ v_\phi}{r^2} \tag{2.40}$$

In the right hand side of the last equation, $\int \frac{\partial}{\partial z}\left(\eta\frac{\partial v_\phi}{\partial z}\right) dz = 0$ because we suppose that $\eta\frac{\partial v_\phi}{\partial z}$ vanishes on the bottom and top surfaces of the disk [$Cla07$]. We now want to combine equations (2.39) and (2.40) in such a way that we obtain one equation for the evolution of the surface density $\Sigma\ (r,t)$, thus

$$\frac{\partial}{\partial t}\left(r\Sigma v_\phi\right) + \frac{1}{r}\frac{\partial}{\partial r}\left(\Sigma r^2 v_\phi v_r\right) = \frac{1}{r}\frac{\partial}{\partial r}\left(\Sigma\nu r^3\frac{\partial\Omega}{\partial r}\right) \tag{2.41}$$

The term on the right hand side represents the torques exerted by viscous forces on the gas. We combine the equations (2.39) and (2.41) to eliminate v_r, and using

the assumption (2.18), we get the radial velocity expression

$$v_r = \frac{-3}{\Sigma r^{\frac{1}{2}}} \frac{\partial}{\partial r}\left(\nu \Sigma r^{\frac{1}{2}}\right) \tag{2.42}$$

Substituting in (2.39) to finally give the equation

$$\frac{\partial \Sigma}{\partial t} = \frac{3}{r}\frac{\partial}{\partial r}\left[r^{\frac{1}{2}}\frac{\partial}{\partial r}\left(\nu \Sigma r^{\frac{1}{2}}\right)\right] \tag{2.43}$$

This equation is one of the key equations in accretion disks theory, its temporal evolution is determined only by the kinematic viscosity ν. In general, ν is a function of local variables in the disk, which are Σ, r, and t. So, the equation (2.43) is a nonlinear diffusion equation for Σ, and the viscous evolution of accretion disks depends on the behaviour of viscosity ν. This clearly emphasises the extremely important role of viscosity.

2.6.1 The solution of Keplerian disks with constant viscosity

In order to get the first idea of viscosity effects on the angular momentum transport, and on the disk evolution and structure, let us first consider that the viscosity ν is constant. This assumption makes the equation (2.43) linear for Σ and the disk consists of only one annulus.

So, with ν =constant, equation (2.43) can be solved by separation of variables. We take $\Sigma(r,t) = r^{\beta}T(t).R(r)$, where β is a free parameter we choose at our convenience. Then (2.43) becomes

$$\frac{T'(t)}{T(t)} = \frac{3\nu}{r^{\beta+1}\ R(r)}\frac{\partial}{\partial r}\left[r^{\frac{1}{2}}\frac{\partial}{\partial r}\left(r^{\beta+1}\ R(r)\right)\right] = \text{constant} = -\lambda \tag{2.44}$$

with λ is a positive real number represents the separation constant, it defines the decay rate of the mode.The time function solution is an exponential function, then Σ can be written as $\Sigma(r,t) = r^{\beta}\ e^{-\lambda t}\ R(r)$, hence

$$\frac{d^2R(r)}{dr^2} + \left(2\beta + \frac{3}{2}\right)\frac{1}{r}\frac{dR(r)}{dr} + \beta\left(\beta + \frac{1}{2}\right)\frac{1}{r^2}\ R(r) + \frac{\lambda}{3\nu}R(r) = 0 \tag{2.45}$$

For convenience, we choose $\beta = -\frac{1}{4}$ we find

$$\frac{d^2R(r)}{dr^2} + \frac{1}{r}\frac{dR(r)}{dr} + \left(k^2 - \frac{1}{16r^2}\right)R(r) = 0 \tag{2.46}$$

This differential equation is Bessel equation of order 1/4, with $k^2 = \frac{\lambda}{3\nu}$, the general solution is

$$R(r) = AJ_{1/4}(kr) + BY_{1/4}(kr) \tag{2.47}$$

A and B are constants can be calculated from the boundary conditions. $J_{1/4}(kr)$ is the BesselJ function of order 1/4, defined as

$$J_{1/4}(kr) = \frac{1}{\Gamma\left(\frac{1}{4}+1\right)}\left(\frac{kr}{2}\right)^{1/4} \approx r^{1/4} \tag{2.48}$$

$Y_{1/4}(kr)$ the BesselY function of order 1/4, defined as

$$Y_{1/4}(kr) = \frac{-\Gamma\left(\frac{1}{4}\right)}{\pi}\left(\frac{2}{kr}\right)^{1/4} \approx r^{-1/4} \tag{2.49}$$

We take the solution with vanishing torque at $r = 0$, so it only remains the BesselJ function in the solution (2.47) and the surface density form becomes

$$\Sigma(r,t) = r^{-\frac{1}{4}}\ J_{1/4}(kr)\ e^{-3\nu k^2 t} \tag{2.50}$$

Now, we consider a general initial-value problem and we resolve the initial surface density $\Sigma(r,0)$ into Bessel functions, so

$$\Sigma(r,0) = \int_0^{\infty} f(k)\ r^{-1/4}\ \ J_{1/4}(kr)\ dk \tag{2.51}$$

Thus, the general solution $\Sigma(r,t)$ is then found by evolving the previous relation

$$\Sigma(r,t) = \int_0^\infty f(k)\ r^{-1/4}\ \ J_{1/4}(kr)\ e^{-3\nu k^2 t}\ dk \tag{2.52}$$

then, we need to use Hankel transforms, the transform pair realizes

$$A(r) = \int_0^\infty a(k)\ \ J_\nu(kr)\ (kr)^{1/2}\ dk \tag{2.53}$$

$$a(k) = \int_0^\infty A(r)\ J_\nu(kr)\ (kr)^{1/2}\ dr \tag{2.54}$$

applying this transform to the initial surface density $\Sigma(r,0)$. First, we can write the formula (2.51) as

$$\Sigma(r,0) = r^{-3/4} \int_0^\infty k^{-1/2}\ f(k)\ J_{1/4}(kr)\ (kr)^{1/2}\ dk \tag{2.55}$$

then, the inverse relation is

$$f(k) = k^{1/2} \int_0^\infty s^{3/4}\ \Sigma(s,0)\ \ J_{1/4}(ks)\ (ks)^{1/2}\ ds \tag{2.56}$$

So, the general solution of $\Sigma(r,t)$ can be written in the form of Green-function solution

$$\Sigma(r,t) = \int_0^\infty G(r,s,t)\ \ \Sigma(s,0)\ \ ds \tag{2.57}$$

where the Green function is given by the integral

$$G(r,s,t) = r^{-1/4} s^{5/4} \int_0^\infty J_{1/4}(kr)\ J_{1/4}(ks) k\ e^{-3\nu k^2 t}\ dk \tag{2.58}$$

Thus

$$\Sigma(r,t) = \frac{r^{-1/4} s^{5/4}}{6\nu t}\ \exp\left[-\frac{r^2+s^2}{12\nu t}\right]\ I_{1/4}\left(\frac{rs}{6\nu t}\right) \tag{2.59}$$

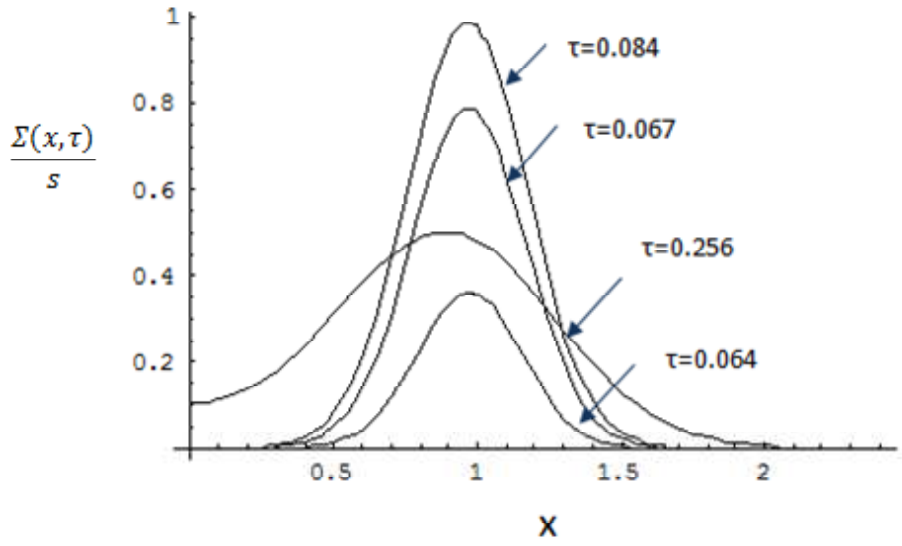

Figure 2.12: The viscous evolution of the surface density Σ of a thin accretion disk ring, for times $\tau = 0.064, 0.067, 0.084, 0.256$.

with $I_{1/4}\left(\frac{rs}{6\nu t}\right)$is the modified Bessel function. To simplify the solution we use the two dimensionless variables $x = r/s$ and $\tau = 12\nu t s^{-2}$, equation (2.59) becomes [$Pri81$],

$$\Sigma\left(x,\tau\right) = \frac{1}{\tau\ x^{1/4}s}\exp\left[-\frac{1+x^2}{\tau}\right] I_{1/4}\left(\frac{2x}{\tau}\right) \tag{2.60}$$

($Fig\ 2-12$) shows the plot of this solution as a function of the dimensionless radius x for a various values of the dimensionless time τ.

We can observe clearly from ($Fig\ 2-12$) why this disk model is always called the spreading ring. This model illustrates what can happen if the disk is under the action of viscous forces, rather than merely accreting, it spreads both inwards and outwards in a complex motion between the matter and angular momentum.

The spread of the matter ring needs a characteristic timescale of order

$$t_{visc} \backsim \frac{r^2}{\nu} \tag{2.61}$$

at each radius r. This relation derived from the equation of radial velocity (2.42) which shows that v_r is of order $v_r \backsim \nu/r$, so the timescale for a radial flow is $t_{visc} \backsim r/v_r \backsim r^2/\nu$. t_{visc} gives an approximation of the time required for the annulus of the disk to move a radial distance r.

When the particles fall and accrete onto an accretion disk, they lean to spiral inwards by losing their energy and angular momentum. So a small amount of matter moves outwards in order to conserve the angular momentum, this leads to outward spreading the shape of the disk. Therefore, at late times, most of the mass is eventually accreted and only the outermost parts of the disk move outwards. For $t \rightarrow \infty$, all the mass in the ring is accreted and the angular momentum is transported to $r \rightarrow \infty$ by a negligibly small amount of mass.

2.6.2 The need for a non-constant viscosity

In the previous model, the value of the kinematic viscosity ν is unkown. We can take values corresponding to viscosities measured for a classical fluids, i.e, the molecular viscosity; is the viscosity due to thermal motion. The molecular viscosity is fairly well known for many materials, it is of the order of 10^{-3} to 10 $cm^2.s^{-1}$ at the room temperature. For exemple, the molecular viscosity of air is 1.5×10^{-1} $cm^2.s^{-1}$, of water 10^{-2} $cm^2.s^{-1}$, of mercury 1.2×10^{-3} $cm^2.s^{-1}$. As the evolutionary models of accretion disks depend strongly on the nature of

viscosity, so when we use the above values to give an estimate of the corresponding viscous timescale, we find values much longer than the Hubble time; the age of the universe $\tau_H \approx 1.3 \times 10^{10} yr$, which indicates that the magnitude of viscosity must be much larger than the standard molecular viscosity. This latter is too low to be responsible for the transport of angular momentum needed in observed disks . Over several years, several modelers have adopted on a very successful parameterization of viscosity in terms of an unknown dimensionless parameter, called α. this prescription has been widely used, it helps us to give a good estimate to the order of magnitude of viscosity.

2.7 The standard model $\ll\alpha$-disk model$\gg$

The standard model was proposed by Shakura and Sunyaev in 1973, it is just a simple parameterization based on dimensional analysis of the viscosity. The basic idea of this theory is that the hydrodynamic turbulence is the cause of an increased turbulent viscosity in the disk. As a consequence of this assumption, we can write the turbulent viscosity ν_{turb} from the equation (1.21) as

$$\nu_{turb} = \frac{1}{3} l_{turb}\ v_{turb} \tag{2.62}$$

with l_{turb} and v_{turb} are respectively the characteristic length and velocity scales of the turbulence. However, both are unknown. The solution of this problem was suggested by Shakura and Sunyaev, they made two assumptions:

First, the length scale equivalent to the thickness H of the disk which is the

largest macroscopic length scale. So l_{turb} is written as

$$l_{turb} = \alpha_l \ H \tag{2.63}$$

where α_l is a constant, smaller or equal to unity.

Second, the turbulent velocity is supersonic and followed by a shock waves that reduce the velocity and dissipate the energy, so v_{turb} is written as

$$v_{turb} = \alpha_\nu \ c_s \tag{2.64}$$

where α_ν is a constant must be smaller or equal to unity too.

Substituting the two equations (2.63) and (2.64) in the equation (2.62) to write the basic assumption of the standard model

$$\nu_{turb} = \frac{1}{3}\alpha_l\alpha_\nu \ c_s \ H = \alpha c_s \ H \tag{2.65}$$

The parameter α is the viscosity constant of Shakura and Sunyaev, $\alpha \leq 1$. Another formalism that is sometimes used is to present the scaling of the viscous stress as

$$W_{r\phi} = \alpha \ P \tag{2.66}$$

with $r\phi$ being the component of the viscous sterss and P is the pressure in the disk.

CHAPTER 3

Steady-state solutions

The stationary state does not mean that there is no flow, but it means that the time derivatives of the fluid properties (velocity v, density ρ, temperature T..) vanish because these quantities remain unchanged. This state is not totally real, but it gives results that have a good agreement with the observation. It is also an important start in the analysis of the complex structure of accretion disks. Many researches suggested that this approximation is verified in the inner regions of the disk because the gas flows with a constant accretion rate.

In section 1, we describe briefly the disks structure in the steady state and we define the equations that control this state. Then, we build a simple model of steady and thin disk around a white dwarf in cataclysmic variable,and we try to recognise the structure of this object from the solution of steady accretion disk equations.

In section 2, we discuss a more complex case, the thick disks.

3.1 Steady thin disks

3.1.1 The structure of steady thin disks

To treat the stationary state of any accretion disk, we set the time-dependent part equal to zero in conservation equations, so the stationary continuity equation

(2.39) becomes

$$\frac{1}{r}\frac{\partial\left(\rho r v_r\right)}{\partial r}=0 \tag{3.1}$$

Substituting the formula (2.19) in (3.1) with the integration, we get

$$r v_r \Sigma = C_1 \tag{3.2}$$

with C_1 is the integration constant, it represents the radial mass flow rate per unit time, hence

$$\dot{M}= 2\pi r\Sigma(-v_r) \tag{3.3}$$

The negative sign has been chosen because the radial velocity v_R is negative (inwards direction). This definition of $\dot{M}$ $[g.s^{-1}]$ is not only used in the stationary case but in general definition as well, but the difference is to be a constant in steady case.

Analogously, from the angular momentum equation (2.40), we get

$$\Sigma r^3\Omega\ v_R - \nu\Sigma r^3\frac{d\Omega}{dr} = C' \tag{3.4}$$

Then, substituting the equation (3.3), we get

$$-\ \dot{M}\ r^2\Omega - 2\pi\nu\Sigma r^3\frac{d\Omega}{dr} = 2\pi C' \tag{3.5}$$

In this equation, the first term on the left-hand side represents the angular momentum advected with the accretion process and the second term indicates the viscous torque exerted by the star on the disk. The integration constant C' represents the net flux of angular momentum or the couple exerted by the star on the inner edge of the disk. So, to determine it we need to consider an inner

boundary condition for the disk. The constant $C^{'}$ determined by assuming that the disk extends to connect with the central object, hence $r = r_*$ and $\frac{d\Omega}{dr} = 0$ (because the angular velocity Ω becomes very close to the Keplerian value Ω_K), therefore, the viscous torque vanishes, [$Fra02$], and equation (3.5) becomes

$$C' = \frac{-\dot{M}\, r_*^2 \Omega_K}{2\pi} = \frac{-\dot{M}}{2\pi}(GMr_*)^{\frac{1}{2}} \tag{3.6}$$

Substituting this into equation (3.4), we get

$$\Sigma r^{3/2} v_r + \frac{3\nu\Sigma}{2} r^{1/2} = \frac{-\dot{M}}{2\pi} r_*^{1/2} \tag{3.7}$$

where we set $\Omega = \Omega_K$. Using (3.3) we find

$$\nu\Sigma = \frac{\dot{M}}{2\pi}\left[1 - (\frac{r_*}{r})^{\frac{1}{2}}\right] \tag{3.8}$$

This formula gives the linear dependence between the viscosity and the surface density with the accretion rate, for steady disks with a slowly rotating star (where $\Omega = \Omega_K$). Although, this is an important result, there are cases where it is not valid, when the disk does not realise the above conditions. We place now this result in equation (2.35) to find the energy flux through the faces of the steady thin disk

$$D(r) = \frac{3GM\,\dot{M}}{8\pi r^3}\left[1 - (\frac{r_*}{r})^{\frac{1}{2}}\right] \tag{3.9}$$

This formula is independent from viscosity when the accretion rate $\dot{M}$ be constant, it is important because it uses to find the total luminosity produced by the disk. By integrating over the whole disk surface by assuming that the disk extends to infinity, we have the disc luminosity

$$L_{disk} = 2\int_{r_*}^{\infty} (2\pi r)\; D(r)\; dr \tag{3.10}$$

Here, we added the factor 2 because we need to calculate the luminosity produced from both sides of the disk. Substituting the expression (3.9), we get

$$L_{disk} = \frac{3GM\ \dot{M}}{2}\left[\int_{r_*}^{\infty}\frac{1}{r^2}dr - \int_{r_*}^{\infty}(\frac{r_*}{r^5})^{\frac{1}{2}}dr\right] \tag{3.11}$$

Hence,

$$L_{disk} = \frac{GM\ \dot{M}}{2r_*} = \frac{1}{2}L_{acc} \tag{3.12}$$

This result is similar to our old result in equation (2.4), where $GM\ \dot{M}\ /r_*$ is the rate of gravitational energy loss due to the accretion process at the surface of the star. Therefore, this equation proves that the luminosity is only half of the potential energy and it is emitted from the disk. The rest energy remains as kinetic energy needed to keep the disk in Keplerian rotation that is radiated after from the boundary layer.

Finally, Let us summarize what have been found so far. Thus, we collect the equations that describe the evolution of steady and thin accretion disks in the following

$$\rho = \frac{\Sigma}{H} \tag{3.13}$$

$$H = \frac{c_s}{\Omega_K} \tag{3.14}$$

$$c_s^2 = \frac{K}{\mu m_p}T \tag{3.15}$$

$$P = \frac{\rho KT}{\mu m_p} \tag{3.16}$$

$$\frac{4\sigma T^4}{3\Sigma\kappa_R} = \frac{3GM\ \dot{M}}{8\pi r^3}\left[1-(\frac{r_*}{r})^{\frac{1}{2}}\right] \tag{3.17}$$

$$\nu\Sigma = \frac{\dot{M}}{2\pi}\left[1-(\frac{r_*}{r})^{\frac{1}{2}}\right] \tag{3.18}$$

3.1.2 The solutions of steady and thin α-disks

Now, we will solve the previous equations with imposing that the viscosity given by the standard model is

$$\nu = \alpha H c_s \tag{3.19}$$

To specify our model, we need to give the form of the opacity, we utilise the analytical form of Kramer (2.31), and to simplify the calculation we set $\left[1-(\frac{r_*}{r})^{\frac{1}{2}}\right] = f^4$, and $\frac{3GM\dot{M}}{8\pi r^3}\left[1-(\frac{r_*}{r})^{\frac{1}{2}}\right] = D$. From (3.15), (3.18) and (3.19), we get the surface density form

$$\Sigma = \left(\frac{\mu m_p}{3\pi K} G^{1/2}\right) \alpha^{-1}\ \dot{M}\ M^{1/2}\ r^{-3/2}\ f^4\ T^{-1} \tag{3.20}$$

and from (3.13), (3.14) and (3.15) we get the density form

$$\rho = \left(\frac{\mu m_p}{K} G\right)^{1/2} \Sigma\ M^{1/2}\ r^{-3/2}\ \ T^{-1/2} \tag{3.21}$$

Now, we place this two forms into the equation of temperature (3.17), we get

$$T = \left[\left(\frac{3G}{8\pi}\right)\frac{3\kappa_0}{4\sigma}\left(\frac{\mu m_p}{K} G\right)^{1/2}\right]^{1/8} \Sigma^{1/4}\ \dot{M^{1/8}}\ M^{3/16}\ r^{-9/16}\ f^{1/2} \tag{3.22}$$

Then, we place this result into the equation (3.20), we obtain

$$\Sigma = A^{4/5}\ \alpha^{-4/5}\ \dot{M^{7/10}}\ M^{1/4}\ r^{-3/4}\ f^{14/5} \tag{3.23}$$

where A is a constant equals to

$$A = \left(\frac{\mu m_p}{3\pi K} G^{1/2}\right)\left[\left(\frac{3G}{8\pi}\right)\frac{3\kappa_0}{4\sigma}\left(\frac{\mu m_p}{K} G\right)^{1/2}\right]^{-1/8} = 4.74\times 10^{-15} \tag{3.24}$$

Then, the other solutions followed with some calculation, we find

$$T = B\ \alpha^{-1/5}\ \dot{M^{3/10}}\ M^{1/4}\ r^{-3/4}\ f^{6/5} \tag{3.25}$$

$$H = C\ \alpha^{-1/10}\ \dot{M^{3/20}}\ M^{-3/8}\ r^{9/8}\ f^{3/5} \tag{3.26}$$

$$\rho = D\ \alpha^{-7/10}\ \dot{M^{11/20}}\ M^{5/8}\ r^{-15/8}\ f^{11/5} \tag{3.27}$$

$$\tau = E\ \alpha^{-4/5} M^{1/5}\ f^{4/5} \tag{3.28}$$

$$\nu = F\ \alpha^{4/5}\ \dot{M^{3/10}}\ M^{-1/4}\ r^{3/4}\ f^{6/5} \tag{3.29}$$

$$v_r = -G\ \ \alpha^{4/5}\ \dot{M^{3/10}}\ M^{-1/4}\ r^{-1/4}\ f^{-14/5} \tag{3.30}$$

where we use the equation (2.42) to give v_r. B, C, D, E, F and G which are constants given by

$$B = A^{-4/5}\left(\frac{\mu m_p}{3\pi K} G^{1/2}\right) = 8.1 \times 10^{-2} \tag{3.31}$$

$$C = A^{-2/5}\,(3\pi)^{-1/2}\,G^{-1/4} = 1.08 \times 10^{7} \tag{3.32}$$

$$D = \frac{A^{4/5}}{C} = 3.199 \times 10^{-19} \tag{3.33}$$

$$E = \kappa_0\ A^{4/5} B^{-7/2}\ D = 3.66 \times 10^{-2} \tag{3.34}$$

$$F = \frac{A^{-4/5}}{3\pi} = 3.05 \times 10^{10} \tag{3.35}$$

$$G = \frac{A^{-4/5}}{2\pi} = 4.57 \times 10^{10} \tag{3.36}$$

Then, we treat the time independent bihaviour of mass transferring binaries, we apply the above equations on a white dwarf of mass $M \simeq 1M_{\odot}$ and radius $r_* \simeq 10^9 cm$, with a constant accretion rate $\dot{M}= 5 \times 10^{16} g.s^{-1}$ coming from the secondary star as a stream of matter. We selected these numerical values to verify

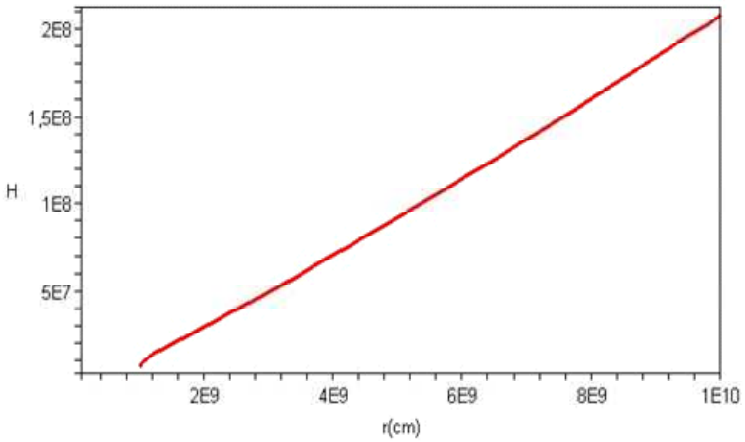

Figure 3.1: The scale-height evolution as a function of the radius r.

our results by the comparison with [$Bat81$], and we chose the cataclysmic binaries for the following reasons:

$*$ Accretion process is the natural consequence of mass transfer in interacting binary stars, and in most of them, the energy output at all the wavelengths spectrum is dominated by this process.

$*$ They are good candidates for testing simple ideas about thin disk approximation, because radiation pressure is unimportant.

In this case, we neglect the effect of mass-transfer-rate bursts because we consider a constant accretion rate, and we also do with the tidal effect exerted by the companion star. Taking $\alpha = 0.4$ and the radius of the disk in the range $10^9 cm - 10^{10} cm$, using these numerical values to complete steady disk solutions,

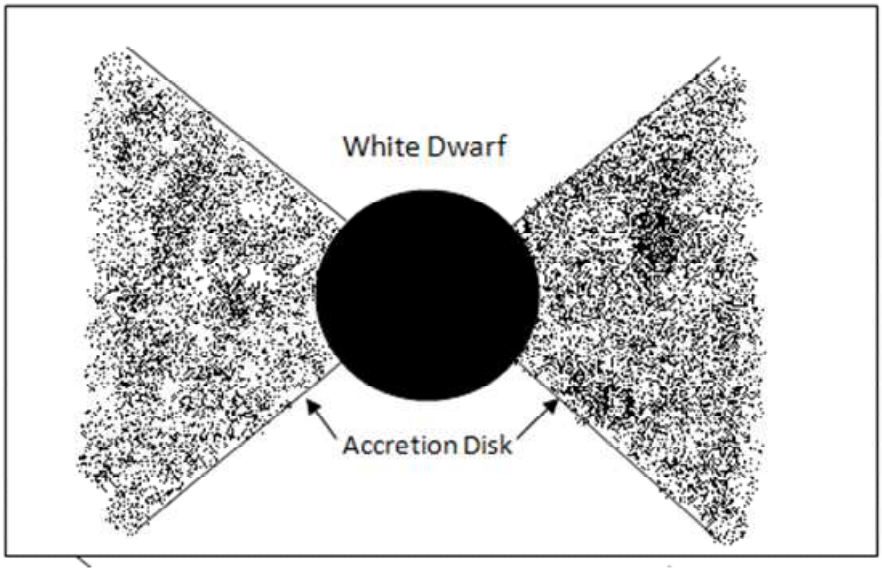

Figure 3.2: Section in disk around a white dwarf, shows the concave shape.

hence

$$\Sigma = 7.47 \times 10^{8}\ r^{-3/4}\left[1-\left(\frac{r_*}{r}\right)^{1/2}\right]^{7/10} \qquad g.cm^{-2} \tag{3.37}$$

$$H = 1.24 \times 10^{-3}\ r^{9/8}\left[1-\left(\frac{r_*}{r}\right)^{1/2}\right]^{3/20} \qquad cm \tag{3.38}$$

$$\rho = 6.02 \times 10^{11}\ r^{-15/8}\left[1-\left(\frac{r_*}{r}\right)^{1/2}\right]^{11/20} \qquad g.cm^{-3} \tag{3.39}$$

$$T = 2.103 \times 10^{12}\ r^{-3/4}\left[1-\left(\frac{r_*}{r}\right)^{1/2}\right]^{3/10} \qquad K \tag{3.40}$$

$$\tau = 1.66 \times 10^{2}\left[1-\left(\frac{r_*}{r}\right)^{1/2}\right]^{1/5} \tag{3.41}$$

$$\nu = 7.102 \times 10^{6}\ r^{3/4}\left[1-\left(\frac{r_*}{r}\right)^{1/2}\right]^{3/10} \qquad cm^2.s^{-1} \tag{3.42}$$

$$v_r = -1.06 \times 10^{7}\ r^{-1/4}\left[1-\left(\frac{r_*}{r}\right)^{1/2}\right]^{-7/10} \qquad cm.s^{-1} \tag{3.43}$$

Now, we represent the previous solutions by the computational software program <<Maple>>. The evolution of some flow properties is shown schematically in figures (3.1, 3.3, 3.5, 3.6, 3.7 and 3.8).

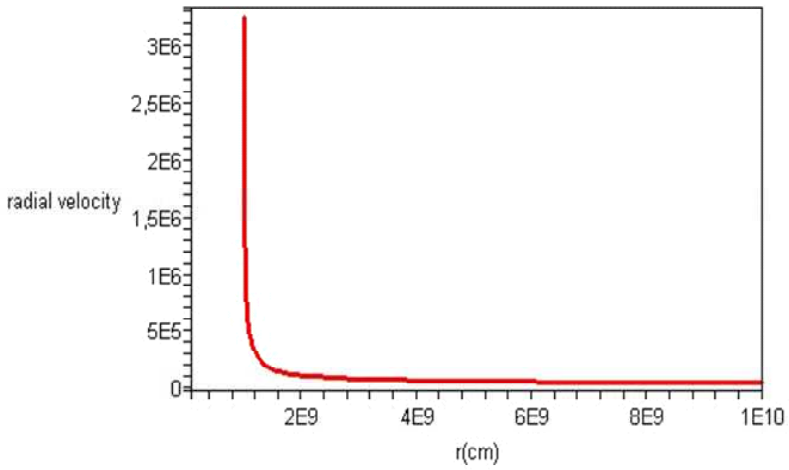

Figure 3.3: The velocity evolution as a function of the radius r.

We note from $(Fig\ 3-1)$ that the disk thickness changes from 10^7 to $10^8 cm$, and the ratio H/r as

$$H/r \approx \alpha^{-\frac{1}{10}}\ r^{1/8} \approx 10^{-2} \tag{3.44}$$

This implies that $H \ll r$, which supports the hypothesis that the disk is geometrically thin. As well as H increases with the radius r and decreases with α, but the decrease is more slower compared to the increase. So, we can conclude the disk shape by using $(Fig\ 3-1)$ which displays a part of the disk form as a function of r, the disk takes a concave shape $(Fig\ 3-2)$.

The negative sign that appears in the radial velocity equation (3.43) shows that the particles move in the opposite direction, the inward radial direction. From $(Fig\ 3-3)$, we note that particles begin the movement with low radial velocity,

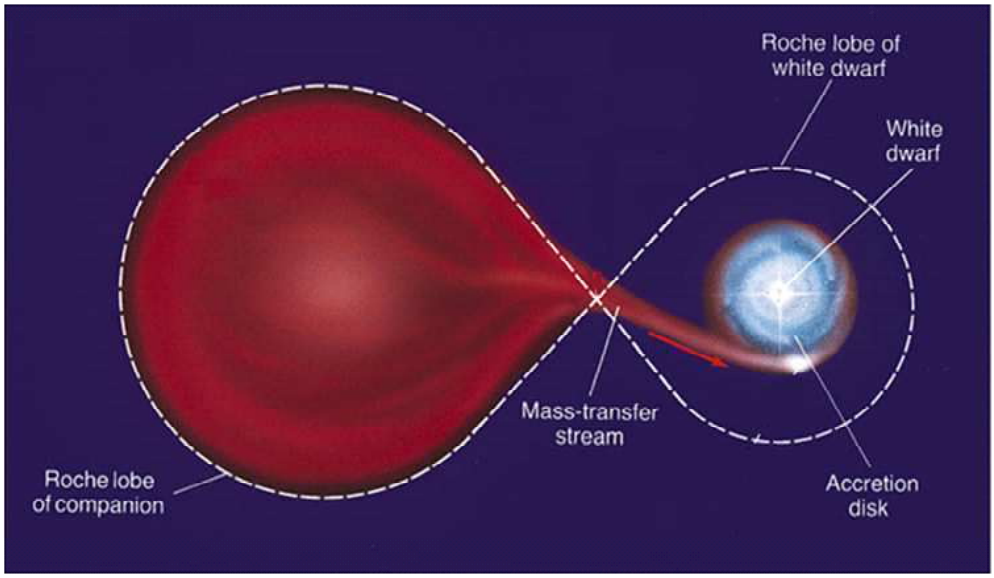

Figure 3.4: Diagram shows the Roch lobe in cataclysmic variable.

but when they approach the star, they take the maximum value where they are under the influence of gravitational field of the star and also because they lose their angular momentum, this latter helps the particles to remain stable. Moreover, the sound speed of this disk ranging from $\backsim 16-28\ km.s^{-1}$, and the Keplerian angular velocity between $1000-2500\ km.s^{-1}$, while the Mach number is $\mathcal{M} \backsim 62-89$, i.e. c_s is much less than v_ϕ and the velocity flow is Hypersonic.

In this steady solution, we take the opacity according to the Kramer law, where it is valid for temperature below to $10^4 K$. We apply this condition to the temperature equation (3.40) and we find

$$r \leq 10^{11} cm \tag{3.45}$$

This means that our solution is broken if the disk extends out to $r > 10^{11} cm$, it quites the Roch Lobe ($Fig\ 3-4$), and stops the accretion process.

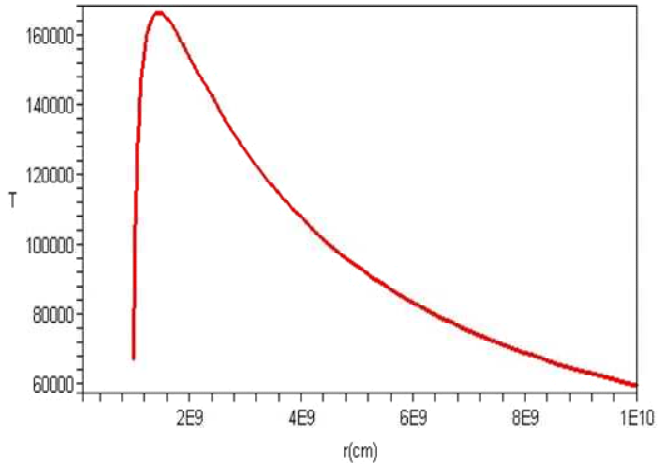

Figure 3.5: The temperature evolution as a function of the radius r.

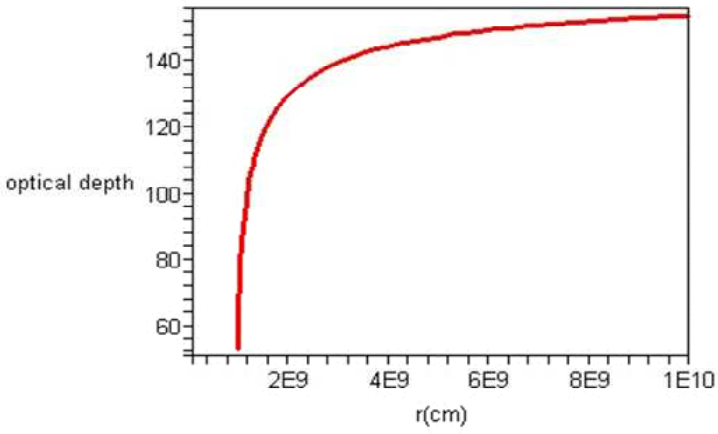

Figure 3.6: The optical depth evolution as a function of the radius r.

($Fig\ 3-5$.) displays that the temperature of the disk varies from 6×10^4 to 16×10^4K, with a small ratio$\backsim$ 2.66, hence the disk temperature is almost uniform from the center to the surface. As we said before that we deal with Kramer opacity law, as it is consistent with the hypothesis of ignoring the radiation pressure. For this law, we need a disk temperature $\leq 10^4K$, but our temperature solution gives values more than this limit. This is due to the value of the accretion rate used (we recall that we used this value to compare the validity of this solution with [$Bat81$]), but when we used values of accretion rate lower than $10^{16}\ g.s^{-1}$, we found temperature solutions less than 10^4K.

So, we conclude that for regions with high accretion rate $\left(\dot{M}> 10^{16}g.s^{-1}\right)$, the temperature degrees rise to be more than 10^4K, and the ionization degree increases too, to support the radiation pressure and the electron scattering (Thomson opacity). These regions can generally exist in disks around neutron stars and black holes. These results supported by [$Sha73$].

From ($Fig3-6$) and the expression of the optical depth (3.41), we observe that the disk is surely optically thick for any value of the accretion rate because it achieves the condition $\tau\gg1$.

($Fig\ 3-7$) shows the evolution of Σ for different values of α, we can see that the difference between the three curves is not remarkable as we will find in the time-dependent case. Also, the viscosity enters almost in all precedent solutions, but with an order of magnitude not sensitive, it does not make a significant change in the disk structure, because of this, the study of viscosity effect on accretion disks

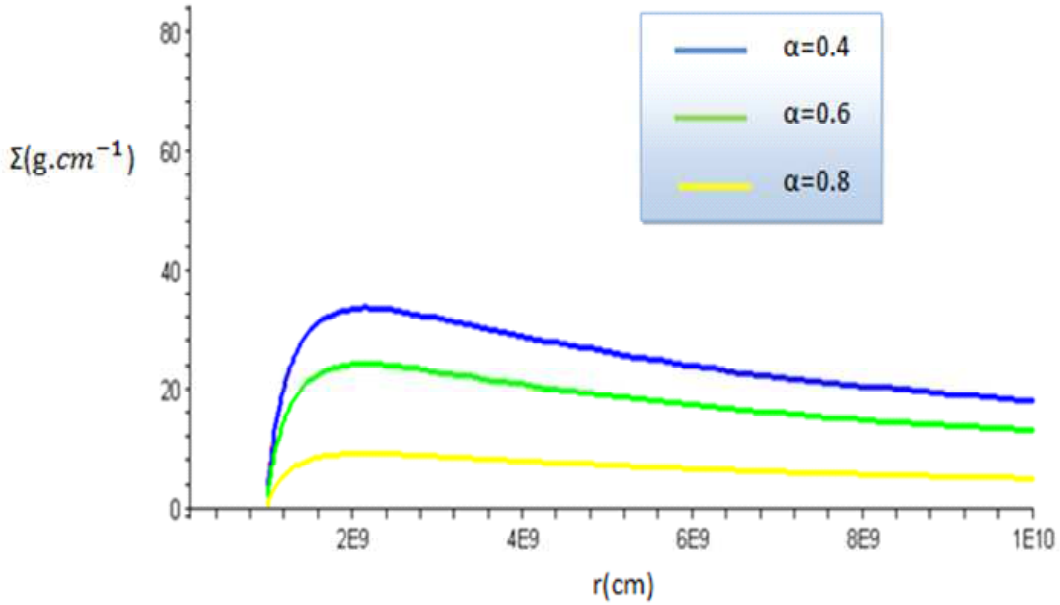

Figure 3.7: The evolution of the surface density as a function of the radius r, for three values of α.

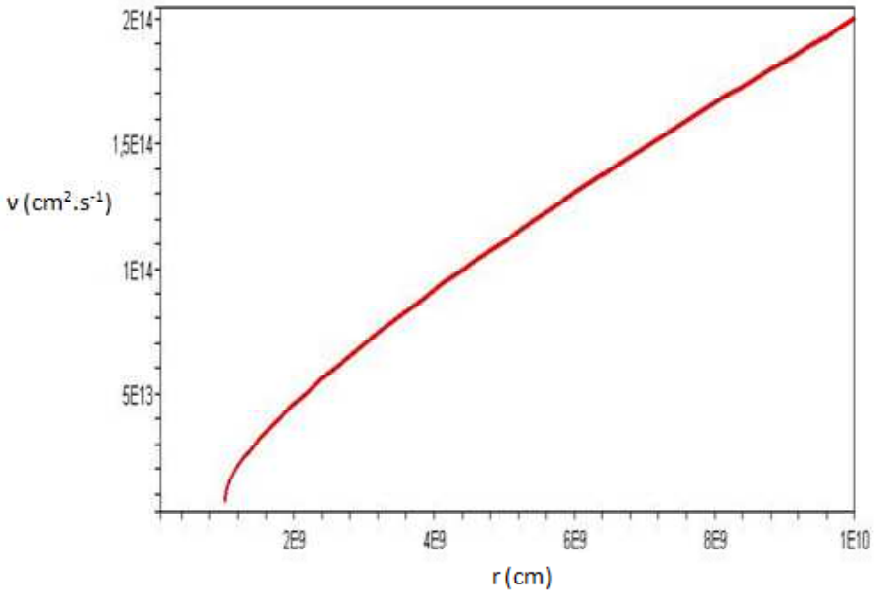

Figure 3.8: The evolution of the kinematic viscosity as a function of the radius r.

has no importance in steady state.

But this does not negate to note from the figure that, as the viscosity increases with radius, the disk rings spread out .

All results which we have found before are comparable with [$Bat81$], where they found that the maximum value of the surface density at the inner radius is $\Sigma = 40\ g.cm^{-1}$, of the thickness $H = 2.1 \times 10^9 cm$ with the ratio $H/r \approx 2.5 \times 10^{-2}$ and of the temperature $T = 5 \times 10^4 K$. These results are supported by the observation too, that considers the gas temperatures in disks around white dwarfs are several $10^4 K$ and the thickness is ranging from 10^7 to $10^9\ cm$.

3.2 Steady thick disks

3.2.1 General formulation

The objective of this section is to explore some of the physical properties of thick accretion disks. First, let us summarize some of the important equations that describe the structure of the disk in this case. This theory is based on the assumption that the disk is in hydrostatic equlibruim outside a certain radius r_{in} (the inner disk radius), and its rotational velocity is not Keplerian. That means that the radial and vertical velocity components are much smaller than the speed of sound. In the following, we shall consider a thick torus around an isolated star which is in the gravitational field of a black hole. Further, to describe the relativistic effects which are important for accretion disks around black holes, we use the pseudo-Newtonian potential instead of using the general relativity. The

form of this potential proposed by Paczyński and Wiita (1980) and given by

$$\Phi = \frac{-GM}{R - r_g} \tag{3.46}$$

with r_g is the gravitational radius, it is chosen equal to the Schwarzschild radius, so $r_g = 2GM/c^2$. R is the spherical radial coordinate, it gives the total distance from the origin to a point on the surface of the disk, $R = (r^2 + z^2)^{1/2}$ with r and z are cylindrical coordinates.

The equation of hydrostatic equilibrium has the form

$$\frac{1}{\rho}\nabla P = -\nabla\Phi - \frac{1}{2}\nabla\left(\Omega^2 r^2\right) + \Omega\nabla\left(\Omega r^2\right) \tag{3.47}$$

In this case of disks, we use the continuity equation (2.12) and the three components of Navier-Stokes equations (2.13), (2.14) and (2.15), taking into account that the effective gravity is the vectorial sum of gravitational and centrifugal acceleration, so

$$g_{eff} = -\nabla\Phi + \Omega^2 r \tag{3.48}$$

In thin disks study, we have been assumed that the vertical velocity $v_z = 0$, and the derivative $\frac{\partial}{\partial z} = 0$, this means that we have a strict cylindrical symmetry. The most realistic assumption is that v_z and v_r change as $v_z \backsim (H/r)\, v_r$ and $\frac{\partial}{\partial z} \backsim (H/r)\, \frac{\partial}{\partial r}$ [$Fra02$], so with this approximation we can neglect all terms containing v_z and z derivatives in the continuity and Navier-Stokes equations. Equation (2.12) becomes

$$\frac{\partial}{\partial r}\left(\rho r v_r\right) + H\frac{\partial}{\partial r}\left(\frac{\rho H}{r} v_r\right) = 0 \tag{3.49}$$

and the three equations (2.13), (2.14) and (2.15) become respectively

$$r \quad : \quad \rho\left\{v_r\frac{\partial v_r}{\partial r}+\left(\frac{H}{r}\right)^2 v_r\frac{\partial v_r}{\partial r}-\frac{v_\phi^2}{r}\right\}=-\frac{\partial P}{\partial r}+\rho g_{eff_r}+\frac{\partial}{\partial r}\left(\eta\frac{\partial v_r}{\partial r}\right) \tag{3.50}$$
$$+\frac{H}{r}\frac{\partial}{\partial r}\left(\frac{\eta H}{r}\frac{\partial v_r}{\partial r}\right)+\frac{1}{r}\frac{\partial}{\partial r}\left(\eta v_r\right)-\eta\frac{v_r}{r^2}$$

$$\phi \quad : \quad \rho\left\{v_r\frac{\partial v_\phi}{\partial r}+\left(\frac{H}{r}\right)^2 v_r\frac{\partial v_\phi}{\partial r}+\frac{v_r v_\phi}{r}\right\}=\rho g_{eff_\phi}+\frac{\partial}{\partial r}\left(\eta\frac{\partial v_\phi}{\partial r}\right) \tag{3.51}$$
$$+\frac{H}{r}\frac{\partial}{\partial r}\left(\frac{\eta H}{r}\frac{\partial v_\phi}{\partial r}\right)+\frac{1}{r}\frac{\partial}{\partial r}\left(\eta v_\phi\right)-\eta\frac{v_\phi}{r^2}$$

$$z \quad : \quad \rho\left\{v_r\frac{\partial}{\partial r}\left(\frac{Hv_r}{r}\right)+\left(\frac{H}{r}\right)^2 v_r\frac{\partial}{\partial r}\left(\frac{Hv_r}{r}\right)\right\}=-\frac{\partial P}{\partial z}+\rho g_{eff_z}$$
$$+\frac{\partial}{\partial r}\left(\eta\frac{\partial}{\partial r}\left(\frac{Hv_r}{r}\right)\right)+\frac{H}{r}\frac{\partial}{\partial r}\left(\eta\frac{H}{r}\frac{\partial}{\partial r}\left(\frac{Hv_r}{r}\right)\right)+\frac{1}{r}\frac{\partial}{\partial r}\left(\eta\frac{Hv_r}{r}\right) \tag{3.52}$$

3.2.2 Resolution of the disk equations

From the previous section, we notice that all the disk equations depend on $\Omega(r)$. Wherefore, we need to specify the angular velocity $\Omega(r)$ only as a function of the position coordinate r, according to the Von Zeipel theorem for the polytropic state equation. This velocity must realize the condition $(d\Omega\,(r)\,/dr<0)$ for the inward accretion. Hence we choose

$$\Omega\,(r)=\frac{\Omega_0}{r^{3/2}}\exp(-\lambda r) \tag{3.53}$$

where it is equal to the Keplerian velocity if $\lambda=0$, and the constant $\Omega_0=\sqrt{GM}$. Therefore, the specific angular momentum is given by

$$j\,(r)=r^2\Omega\,(r)=\Omega_0 r^{1/2}\exp(-\lambda r) \tag{3.54}$$

Radial velocity

Now, we deal with the assumption that the radial velocity is slowly changing with r meaning that

$$\frac{\partial v_r}{\partial r} = 0 \tag{3.55}$$

Therefore, the conservation equation (3.50) becomes

$$v_r = \frac{-\frac{\partial P}{\partial r} + \rho\left[g_{eff_r} + \frac{\Omega_0^2 \exp(-2\lambda r)}{r^2}\right]}{\frac{\eta}{r^2} - \frac{1}{r}\frac{\partial \eta}{\partial r}} \tag{3.56}$$

The surface density

By the application of the condition (3.55), the equation (3.51) becomes

$$\begin{aligned} & \rho\left\{v_r\left[\left(\Omega(r) + r\frac{\partial \Omega(r)}{\partial r}\right)\left(1 + \left(\frac{H}{r}\right)^2\right) + \Omega(r)\right] - g_{eff_\phi}\right\} \\ = \; & 2\Omega(r)\frac{\partial \eta}{\partial r} + \frac{\partial \Omega(r)}{\partial r}\left(3\eta + r\frac{\partial \eta}{\partial r}\right) + r\eta\frac{\partial^2 \Omega(r)}{\partial r^2} + \frac{H}{r} \times \\ & \left[\frac{\partial^2 \Omega(r)}{\partial r^2}(\eta H) + \frac{\partial \Omega(r)}{\partial r}\left(\frac{\eta H}{r} + \eta\frac{\partial H}{\partial r} + H\frac{\partial \eta}{\partial r}\right)\right] \\ & + \frac{H\Omega(r)}{r^2} \times \left[H\frac{\partial \eta}{\partial r} + \eta\frac{\partial H}{\partial r} - \frac{\eta H}{r}\right] \end{aligned} \tag{3.57}$$

After some calculations we can find the surface density equation, which is

$$\begin{aligned} & \Sigma v_r\left\{\frac{1}{2Hr} - \frac{\lambda}{H} - \frac{H}{2r^3} - \frac{H\lambda}{r^2} - \frac{\Omega_0 \exp(-\lambda r)}{r^{3/2} H v_r}\right\} \\ = \; & \frac{\partial H}{\partial r} \times \left[\frac{H\eta}{r^2}\left(\lambda - \frac{1}{2r}\right)\right] - \frac{\partial \eta}{\partial r}\left[\left(\frac{H}{r}\right)^2\left(\frac{1}{2r} + \lambda\right) - \frac{1}{2r} + \lambda\right] \\ & + \eta\left[\left(\frac{H\lambda}{r}\right)^2\left(1 + \frac{2}{\lambda r} + \frac{5}{4r^2\lambda^2}\right) + \left(\frac{1}{\eta r} - \frac{3}{4r^2} + \lambda^2\right)\right] \end{aligned} \tag{3.58}$$

The surface equation

1-the approximate expression: Since the main objective of the study of thick accretion disks is to know the shape of the disk, we use the continuity equation (3.49) to find the expression of H. We place the equation (2.19) in (3.49), we find

$$\frac{\partial}{\partial r}\left(\frac{\Sigma r v_r}{H}\right)+H\frac{\partial}{\partial r}\left(\frac{\Sigma v_r}{r}\right)=0 \tag{3.59}$$

Supposing that the accretion rate is constant, $\dot{M}=-2\pi r v_r\Sigma$ =constant, so equation (3.59) becomes

$$\frac{\partial}{\partial r}\left(\frac{-\dot{M}}{2\pi H}\right)+H\frac{\partial}{\partial r}\left(\frac{-\dot{M}}{2\pi r^2}\right)=0 \tag{3.60}$$

Thus

$$\frac{\partial}{\partial r}\left(\frac{1}{H}\right)+H\frac{\partial}{\partial r}\left(\frac{1}{r^2}\right)=0 \tag{3.61}$$

Finally we get the following differential equations

$$\frac{\partial H}{\partial r}+\frac{2H^3}{r^3}=0 \tag{3.62}$$

The solution of this equation is given as

$$H\left(r\right)=\frac{1}{\sqrt{2a}}\frac{r}{\sqrt{r^2-\frac{1}{a}}} \tag{3.63}$$

($Fig\ 3-9$) represents the evolution of the disk thickness but with an approximative method, the following calculations will give us a more accurate information about the disk shape.

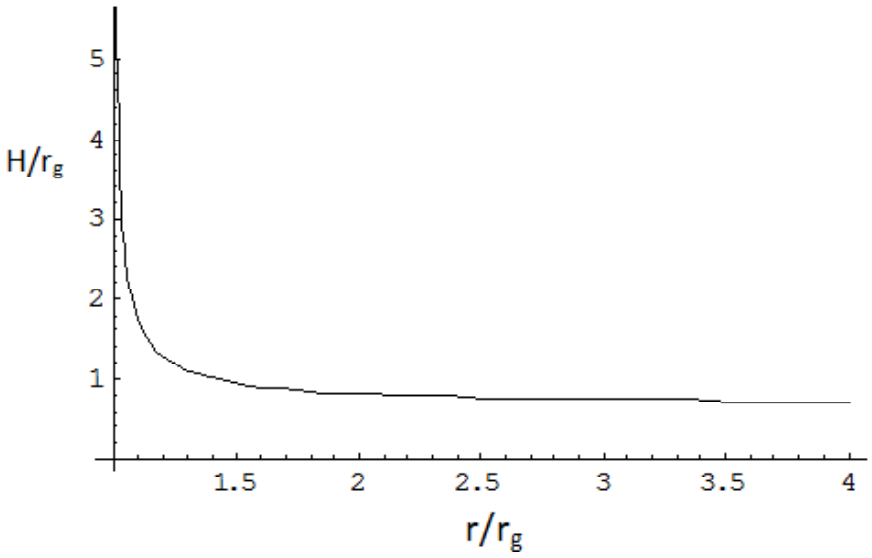

Figure 3.9: The evolution of the disk thickness.

2-the exact expression: The condition of hydrostatic equilibrium at the disk surface will help us to find the equation of the disk shape. We cosider that $z_0(r)$ is the relation that describes the disk surface, so it verifies the following equation [$Pac80$]

$$\left(\frac{de}{dr}\right)_{z_0(r)} = \left(\frac{dj}{dr}\right)_{z_0(r)} .\Omega\,(r) \tag{3.64}$$

where j is the specific angular momentum, e the specific binding energy and it is given as

$$e = \Phi + \frac{1}{2}v_\phi^2 \tag{3.65}$$

and the derivative of Φ is

$$\left(\frac{d\Phi}{dr}\right)_{z_0(r)} = \left(\frac{\partial\Phi}{\partial r}\right)_{z_0(r)} + \left(\frac{\partial\Phi}{\partial z}\right)_{z_0(r)} \frac{dz_0(r)}{dr} \tag{3.66}$$

substituting in equation (3.64), and after some calculation we find the following differential equation

$$\frac{dz_0(r)}{dr} = \frac{\sqrt{r^2+z_0^2(r)}\left[\sqrt{r^2+z_0^2(r)}-r_g\right]^2}{(GM)\ z_0(r)} \times \left[\frac{-GMr}{\sqrt{r^2+z_0^2(r)}\left[\sqrt{r^2+z_0^2(r)}-r_g\right]^2} + r^2\Omega(r)\left(\frac{d\Omega(r)}{dr}+\frac{\Omega(r)}{r}-1\right)\right] \tag{3.67}$$

This equation describes the variation of the disk surface (the half-thickness) and does not contain any information about the disk interior. Therefore , in the following we study only the variation of the disk surface.

From the vertical component of the (3.47), we find the differential equation of the surface density, this property can be computed by assuming a polytropic equation of state (1.13), we get

$$\rho^{\frac{1}{n}-1}\frac{d\rho}{dr} = \frac{nGM}{K(n+1)\sqrt{r^2+z_0^2(r)}\left[\sqrt{r^2+z_0^2(r)}-r_g\right]^2}\left(z_0(r)\frac{dz_0(r)}{dr}\right) \tag{3.68}$$

With the proposed formula (3.53) of rotational velocity, the surface equation becomes

$$z_0(r)\frac{dz_0(r)}{dr} = -r - \exp(-2\lambda r)\sqrt{r^2+z_0^2(r)}\left[\sqrt{r^2+z_0^2(r)}-r_g\right]^2 \times \left[\frac{2\lambda r+1}{2r^2}+r^{1/2}\exp(\lambda r)\right] \tag{3.69}$$

From now, we present our results in terms of non-dimensional units. We take $GM=1$, r_g the unit of length. Moreover, the last equation becomes,

$$z_0(r)\frac{dz_0(r)}{dr} = -xr_g - \sqrt{x^2+\left(\frac{z_0(r)}{r_g}\right)^2}\left[\sqrt{x^2+\left(\frac{z_0(r)}{r_g}\right)^2}-1\right]^2 \times \left[\frac{\exp(-2\lambda r_g x)(2\lambda r_g x+1)}{2x^2}+\left(r_g^{-3}x\right)^{1/2}\exp(-\lambda r_g x)\right] \tag{3.70}$$

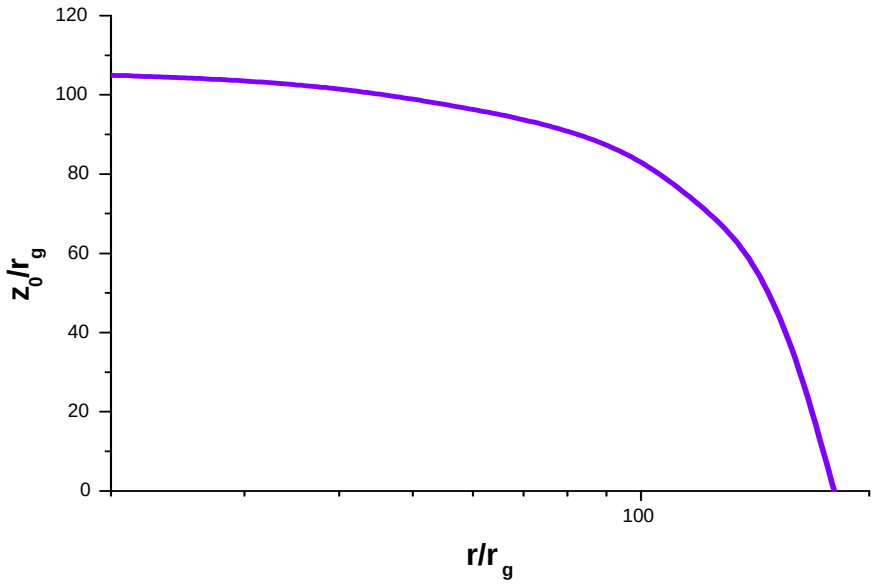

Figure 3.10: Cross section in the $r-z$ plane represent one-half of a Keplerian thick disk.

where $x = r/r_g$.

The second key step is to choose the value of λ. if $\lambda = 0$, the particles move with Keplerian velocity, from this condition we can conclude the nature of the particles motion; it can be sub-Keplerian if $\lambda > 0$ and super-Keplerian if $\lambda < 0$. For the comparision with the results obtained by [$Rub05$], we adopt the sub-Keplerian velocity distribution with $\lambda = 1$.

In order to evaluate the above equations, we must also choose the radius range and the star mass. We take a torus orbiting a $2.5M_{\odot}$ black hole, and the disk radius is chosen according to the supposition of pseudo-Newtonian potential; $r > 3r_g$ ($3r_g$ is the last stable circular orbit).

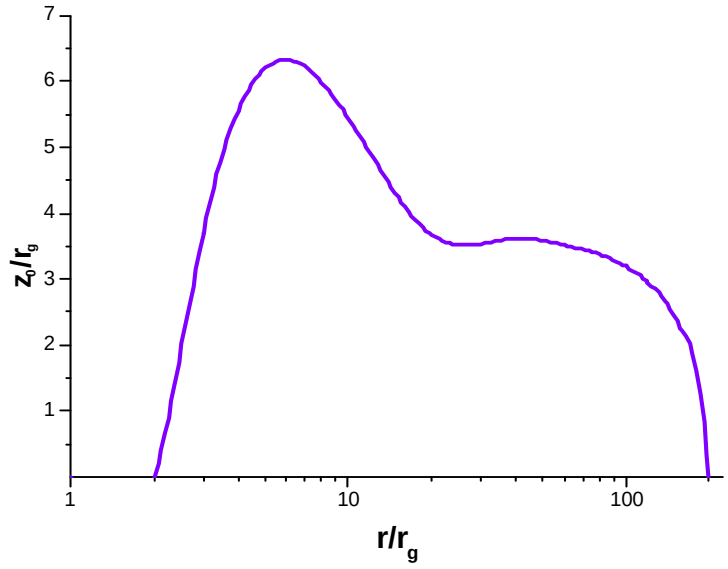

Figure 3.11: Cross section in the $r-z$ plane represent one-half of a non-Keplerian thick disk.

Now, we can solve numerically the equation (3.70), we take the boundary condition that the disk surface $z_0(r) \rightarrow 0$ where $r \rightarrow \infty$, we use the numerical method of Runge-Kutta *RK-45.*

First, we solve the surface equation (3.64) for the Keplerian velocity case, i.e. for $\lambda = 0$, and the solution is represented in $(Fig\ 3-10)$.

The variation in the surface form for a non-Keplerian velocity distribution is shown in $(Fig\ 3-11)$. The small figure in the upper right shows the correct proportion of the disk shape, taken from $[Zur86]$, it shows the funnel opening which is formed near the black hole. It should be noted that as r increases, $z_0(r)$ decreases for $r > 3r_g$, and for $r < 3r_g$.the surface $z_0(r)$ increases with r.

Next, we solve the mass density equation, we take from [$Hor04$],

$$K = \mathcal{R}T\frac{\rho^{-\frac{1}{n}}}{\mu} \tag{3.71}$$

This formula is realised for perfect gases, where $\mathcal{R}$ is the perfect gas constant and it is equal to $\mathcal{R}$ =8.3143 $\times 10^7 erg.K^{-1}.mole^{-1}$, T is the disk temperature. In this case, the disk is supported by radiation pressure and electron scattering, we accept that the temperature must be more than $10^4 K$ and the polytropic index $n = 3$. Therefore, in the next calculation, we take $T = 10^5 K$. Now, we place the formula of the angular velocity in the equation (3.68), we find

$$\begin{aligned} \frac{4}{3}\rho^{-\frac{2}{3}}\frac{d\rho}{dr} &= \frac{-r}{\sqrt{r^2+z_0^2(r)}\left[\sqrt{r^2+z_0^2(r)}-r_g\right]^2} - \\ &\quad \exp\left(-2\lambda r\right)\times\left[\frac{2\lambda r+1}{2r^2}+r^{1/2}\exp(\lambda r)\right] \end{aligned} \tag{3.72}$$

Then, substituting the values of n and K and using the non-dimensional units, the recent equation becomes

$$\begin{aligned} \left(1.78\times 10^{13}\right)\rho^{-1}\frac{d\rho}{dr} &= \frac{-x}{r_g\sqrt{r^2+z_0^2(r)}\left[\sqrt{r^2+z_0^2(r)}-r_g\right]^2} \\ &\quad -\frac{\exp\left(-2\lambda r_g x\right)\left(2\lambda r_g x+1\right)}{2\left(r_g x\right)^2}+\left(r_g x\right)^{1/2}\exp\left(-\lambda r_g x\right) \end{aligned} \tag{3.73}$$

The solution of this equation is shown in ($Fig\ 3-12$).

3.2.3 Results and outlooks

In this section, we have performed a model of geometrically thick fluid disk in axisymetric, we have neglected the self-gravity because the disk mass is small

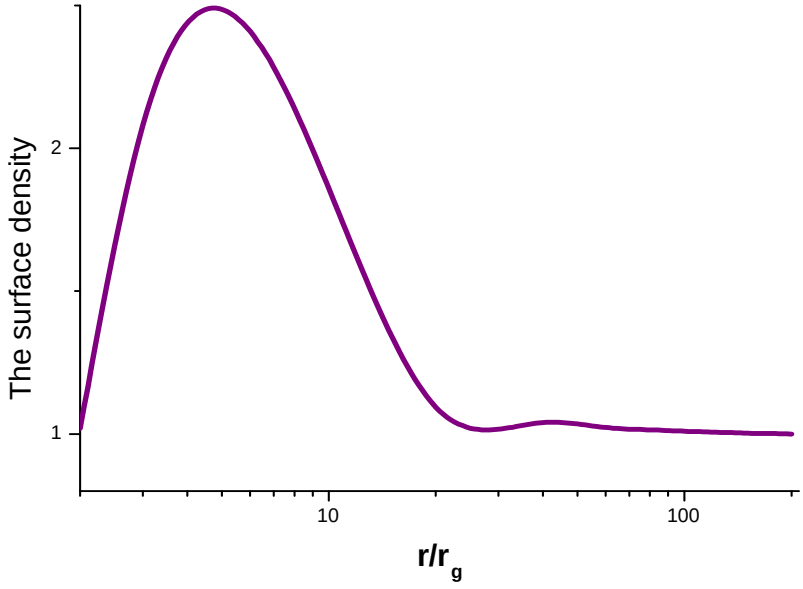

Figure 3.12: The density distribution of thick accertion disk in unit of r_g.

compared to that of the cental object, but we have used a pseudo-Newtonian potential to embody the effect of strong gravity for the potentiel produced by this object. Also, we build initial conditions in hydrostatic equilibrium and we describe the rotation law by giving the distribution of the non-Keplerian angular velocity, a polytropic equation of state has been used. This type of models has been computed by several articles under a number of assumptions (see ref [$Pac80$], [$Lu00$]).

One of the most attractive features in the study of thick accretion disks is the funnel (cusp) forming at the their inner regions (along the rotation axis). This cusp forms particularly due to the large amount of luminosity that can realise in this region and also to the non-Keplerian distribution of angular momentum. The surface curve supports the realization of this theory, and that this cusp is at $3r_g$ and

can extend until $2r_g$ (the marginally bound circular orbit) [$Pac80$]. Close to the rotation axis, the hydrostatic equilibrium breaks down and it becomes not possible because an axial region known as $^{<<}$the disk funnel$^{>>}$ forms, and the matter in this vortex funnel will either fall into the hole or will be thrown by radiation pressure. All this can happen only when a non keplerian angular momentum distribution exists, as is shown in ($Fig\ 3-10$), which represents the surface of thick Keplerian disk with $\lambda = 0$, we can see the non-existence of the disk cusp at its inner edge, and the surface distribution of the disk begins from the center. The surface curve found from the precedent calculation is not totally compatible with the results of [$Rub05$], but it is acceptable and it can show the shape of the disk that must be found.

This shape not realised in the case of thin accretion disks, as we found in the precedent section. The disk can obtain this form when the radiation pressure is the dominent and both accretion rate and luminosity can exceed the normal critical limits.

The shape of the density curve is similar to all models of this type, it indicates that the density exhibits a maximum near the black hole due to the accumulation of the particles in this region, and finally it becomes constant in the outer region.

CHAPTER 4

Time-dependent solutions

In chapter 2, we have seen the effect of viscosity on the evolution of accretion disks by solving the diffusion equation (2.43), with the assumption that the kinematic viscosity ν is constant. In reality, accretion disks do not have a constant viscosity. Therefore, we will resolve the viscous equation (2.43) with another viscosity expression that depends on the two variables, radius r and time t, in addition to the parametre α. Then, we will examine the dynamical (i.e. time-dependent) behaviour for different values of α, and as we shall see for different timing.

The use of this viscosity expression, means that in this model the turbulence is the dominant process for the outward transport of angular momentum, and it makes the equation (2.43) nonlinear, so we will need a numerical solution.

In this chapter, we discuss a model of time-dependent, geometrically thin and optically thick accretion disk with a non constant viscosity, where it resides around a supermassive black hole.

4.1 The characteristic timescales

Before moving on to discuss the time dependent solutions of accretion disks, it is useful to briefly present the various timescales over which they form and evolve. We take into account only the important time scales which are four types:

*The dynamical timescale

The dynamical timescale is the time needed to reach centrifugal equilibrium, this is the shortest characteristic timescale, given by

$$t_{dyn} = \frac{r}{v_\phi} = \Omega^{-1} \tag{4.1}$$

This is also the typical growth time of some important instabilities, such as gravitational and magneto-rotational instability.

*The vertical timescale

The vertical timescale is the time needed to reach the hydrostatic balance in the vertical direction, it evaluates the speed with which hydrostatic equilibrium in the vertical direction is established. Hence

$$t_z = \frac{H}{c_s} = \frac{H}{H\Omega} = \Omega^{-1} = t_{dyn} \tag{4.2}$$

*The viscous timescale

As we have seen in the second chapter, the viscous timescale is given by

$$t_{visc} \backsim \frac{r^2}{\nu} \backsim \frac{r}{v_r} \tag{4.3}$$

t_{visc} is the scale for the evolution of the surface density, so it is the time on which the matter flows from the outer to the inner parts of the disk under the effect of viscous torques. Using the α-prescription for viscosity, we get

$$t_{visc} \backsim \frac{r^2}{\alpha c_s H} \backsim \left(\frac{H}{r}\right)^{-2} \frac{1}{\alpha\Omega} \backsim \alpha^{-1} t_{dyn} \mathcal{M}^2 \tag{4.4}$$

*The Thermal timescale

The thermal timescale is the time needed by the disk to modify its thermal structure, and its temperature. It is defined as follows [$Fra02$]

$$t_{th} = \frac{heat\ content\ per\ unit\ disk\ area}{dissipation\ rate\ per\ unit\ disk\ area} \tag{4.5}$$

thus,

$$t_{th} \backsim \frac{\Sigma\, c_s^2}{D(r)} \tag{4.6}$$

substituting by the formula of the dissipation rate $D(r)$ with $\Omega\,(r) = \Omega_k\,(r)$, we get

$$t_{th} \backsim \frac{\Sigma\, c_s^2}{\nu\Sigma\frac{GM}{r^3}} \backsim c_s^2\, \frac{r}{GM}\frac{r^2}{\nu} \backsim \mathcal{M}^{-2} t_{visc} \tag{4.7}$$

hence,

$$t_{th} \backsim \alpha^{-1} t_{dyn} \tag{4.8}$$

We can see from the previous analyses that the various timescales are ordered in the following way

$$t_{dyn} \backsim t_z \backsim \alpha t_{th} \backsim \alpha\mathcal{M}^{-2} t_{visc} \tag{4.9}$$

thus,

$$t_{visc} \gg t_{th} \gg t_{dyn} \backsim t_z \tag{4.10}$$

This means that the hydrostatic balance in the vertical direction and the centrifugal balance in the radial direction are very rapidly achieved, while the temperature of the disk evolves on a longer timescale.

4.2 Time-dependent thin disks

4.2.1 The viscosity equation

In this case of time-dependent disks, the influence of viscosity on their evolution is more appearing than in the case of steady disks. The inclusion of the turbulent viscosity parameterization in terms of the single parameter α, equation (2.65),

allows us to find another formula for the kinematic viscosity ν that would help us to solve numerically the equation (2.43). To derive the viscosity equation that we will use in time-dependent solution for thin accretion disks. First, we set all the equations that describe their evolution, which are

$$\Sigma = H\ \rho \tag{4.11}$$

$$H = c_s \left(\frac{r^3}{GM}\right)^{1/2} \tag{4.12}$$

$$c_s^2 = \frac{K}{\mu m_p} T \tag{4.13}$$

$$\frac{4\sigma}{3\Sigma\kappa_R} T^4 = \frac{9}{8}\nu\Sigma\frac{GM}{r^3} \tag{4.14}$$

$$\kappa_R = \kappa_0\ \rho^a\ T^b \tag{4.15}$$

$$\nu = \alpha c_s H \tag{4.16}$$

$$\frac{\partial\Sigma}{\partial t} = \frac{3}{r}\frac{\partial}{\partial r}\left(r^{1/2}\frac{\partial}{\partial r}(\nu\Sigma r^{1/2})\right) \tag{4.17}$$

All these equations are derived before. Now, we try to solve this system of equations to get the formula of the viscosity. First, we write respectively the five equations (4.11), (4.12), (4.13), (4.15), and (4.16) in terms of Ω_k, Σ and T, we get [$Del02$]

$$\rho = \Sigma\ \Omega_k \left(\frac{K}{\mu m_p}\right)^{-1/2} T^{-1/2} \tag{4.18}$$

$$H = \Omega_k^{-1}\sqrt{\frac{K}{\mu m_p}} T^{1/2} \tag{4.19}$$

$$c_s = \sqrt{\frac{K}{\mu m_p}} T^{1/2} \tag{4.20}$$

$$\kappa_R = \kappa_0\ \left(\frac{K}{\mu m_p}\right)^{\frac{-a}{2}} \Sigma^a \Omega_k^a T^{b-\frac{a}{2}} \tag{4.21}$$

$$\nu = \alpha \left(\frac{K}{\mu m_p}\right) \frac{T}{\Omega_k} \tag{4.22}$$

Substituting these forms in equation (4.14), we find the temperature equation in terms of Ω_k and Σ, thus,

$$T = \left(\frac{27\alpha\kappa_0}{32\sigma}\right)^{\frac{2}{6-2b+a}} \left(\frac{K}{\mu m_p}\right)^{\frac{2-a}{6-2b+a}} \Sigma^{\frac{2(a+2)}{6-2b+a}} \Omega_k^{\frac{2(1+a)}{6-2b+a}} \tag{4.23}$$

then, we place this result in equation (4.22), using the relation of Keplerian velocity (2.18) to find the equation of ν, we get

$$\nu = \alpha^{\frac{2}{6-2b+a}+1} \left(\frac{27\kappa_0}{32\sigma}\right)^{\frac{2}{6-2b+a}} \left(\frac{K}{\mu m_p}\right)^{\frac{2-a}{6-2b+a}+1} \Sigma^{\frac{2(a+2)}{6-2b+a}} (GM)^{\frac{a+1}{6-2b+a}-\frac{1}{2}} r^{-3\left(\frac{a+1}{6-2b+a}-\frac{1}{2}\right)} \tag{4.24}$$

We can write this relation as

$$\nu = C\ r^p\ \Sigma^q \tag{4.25}$$

with

$$C = \alpha^{\frac{2}{6-2b+a}+1} \left(\frac{27\kappa_0}{32\sigma}\right)^{\frac{2}{6-2b+a}} \left(\frac{K}{\mu m_p}\right)^{\frac{2-a}{6-2b+a}+1} (GM)^{\frac{a+1}{6-2b+a}-\frac{1}{2}} \tag{4.26}$$

and

$$p = -3\left(\frac{a+1}{6-2b+a} - \frac{1}{2}\right) \tag{4.27}$$

$$q = \frac{2\,(a+2)}{6-2b+a} \tag{4.28}$$

Equation (4.25) gives the expression of the viscosity as a power-law formula of r and Σ. We use this relation to find the time-dependent solution of the diffusion equation (4.17) in terms of the constants p and q.

4.2.2 Numerical technique

Starting with solving the surface density equation (4.17), then the rest of the fluid equations, because they all depend on Σ. Using the viscosity form (4.25) to get the effect of the turbulent viscosity at the transport of both, matter and angular momentum in accretion disks evolved with time. To simplify the calculation, we make (4.17) non-dimensional by scaling the variable r with its typical value, a non-dimensional parameter appears $x = \left(\frac{r}{r_0}\right)^{1/2}$. So, the application of this transformation gives

$$\frac{\partial \Sigma}{\partial t} = \frac{3}{4x^3 r_0^2} \frac{\partial^2}{\partial x^2} \left(x \nu \Sigma\right) \tag{4.29}$$

Then, using the method of variables separation, we can write the surface density as

$$\Sigma \left(r, t\right) = T \left(t\right) . X \left(x\right) \tag{4.30}$$

Substituting in equation (4.25), we get

$$\nu = C \ r_0^p x^{2p} \ T^q \left(t\right) \ X^q \left(x\right) \tag{4.31}$$

Now, we place this form with (4.30) in (4.29), we find

$$\frac{T' \left(t\right)}{T^{q+1}(t)} = C' \left(2p \left(2p+1\right) x^{2p-4} X^q \left(x\right) + 2 \left(2p+1\right) \left(q+1\right) x^{2p-3} X^{q-1} \left(x\right) \frac{\partial X \left(x\right)}{\partial x}\right.$$

$$\left. + q \left(q+1\right) x^{2p-2} X^{q-2} \left(x\right) \left(\frac{\partial X \left(x\right)}{\partial x}\right)^2 + \left(q+1\right) x^{2p-2} X^{q-1} \left(x\right) \frac{\partial^2 X \left(x\right)}{\partial x^2}\right) \tag{4.32}$$

with $C' = \frac{3 C r_0^{p-2}}{4}$. Because the left-hand side of equation (4.32) is only function of t and the right-hand side is only function of x, where x and t are independent

variables, the unique way that can hold for all values of x and t is to set each side equal to a constant. Doing so, we get the two differential equations

$$T'(t) + \lambda T^{q+1}(t) = 0 \tag{4.33}$$

and

$$\begin{aligned} & 2p(2p+1)x^{2p-4}X^{q}(x) + 2(2p+1)(q+1)x^{2p-3}X^{q-1}(x)\frac{\partial X(x)}{\partial x} \\ & +q(q+1)x^{2p-2}X^{q-2}(x)\left(\frac{\partial X(x)}{\partial x}\right)^{2} + (q+1)x^{2p-2}X^{q-1}(x)\frac{\partial^2 X(x)}{\partial x^2} + \frac{\lambda}{C'} \\ = \; & 0 \end{aligned} \tag{4.34}$$

λ is the separation constant. The first equation in t is an ordinary first-order differential equation, and the second is an ordinary second-order differential equation. Now, we can find the time solution of the surface density in terms of p and q.

Then, we specify some quantities that are needed to complete the numerical solution, and we use the numerical method Runge-Kutta *RK-45* to solve the equations by the computational software program Maple.

4.2.3 Accretion disks around black holes

The study of accretion disks around black holes has much importance, because these compact objects radiate neither gravitational nor electromagnetic waves, the only way to detect them is by the detection of the emitted radiation from the neighbouring disks or by their impact on the adjoining stars.

Accretion disks are formed around black holes as a natural consequence of the tidal disruption of the nearby stars (there are other mechanisms which can support

in the formation of accretion disks in this stellar case, but this mechanism is the most effective). For this, we suppose that the supplied mass to the disk then to the black hole is only due to the tidal disruption. When a star passes close enough to a supermassive black hole, its tidal gravity exceeds the self-gravity of the star, this leads to pull the matter of this star till it shredes, so a half of the stellar material is ejected and the other half falls onto the black hole. Once the stellar debris are fallen, they begin to rotate in orbits and form an accretion disk. [*Ree*88] was able to make an estimate for the tidal radius in which the star cannot escape, is

$$r_T \simeq r_* \left(\frac{M_b}{M_*}\right)^{\frac{1}{3}} \simeq 1.5 \times 10^{13} \left(\frac{M_*}{M_\odot}\right)^{-\frac{1}{3}} \left(\frac{M_b}{10^7 M_\odot}\right)^{\frac{1}{3}} \left(\frac{r_*}{r_\odot}\right) cm \tag{4.35}$$

where M_b is the black hole mass, r_* and M_* are radius and mass of the incoming star.

In the next calculation, we consider an accretion disk around a non rotating black hole (a Schwarzschild black hole) of mass $M \simeq 10^7 M_\odot$, with the existence of an effective way to remove the angular momentum. The innermost stable orbit must be outside the event horizon in order to take the non-relativistic case, i.e. must be more than three times the Schwarzschild radius (is the radius of the horizon), so $r \geq 3 \times \frac{2GM}{c^2} = 8.84 \times 10^{12} cm$. We choose a $10^7 M_\odot$ black hole becuase many indirect evidences are compatible with the presence of great number of $10^6 - 10^8 M_\odot$ black holes type in the nuclei of many nearby galaxies such as in the center of our galaxy.

We use simple physical assumptions to make the disk sensitive only to the viscosity variation and the black hole is just like a supermassive star, which are

* Neglecting the radial pressure, due to thin approximation.

* Neglecting also the self-gravity effect of the disk because its mass will be much smaller than that of the black hole.

* Taking not into account the relativistic effects.

4.2.4 Initial and boundary conditions

We have to solve two ordinary differential equations for the surface density Σ as a function of x and t. The differential equation of time (4.33) has no solution where the initial condition is $T(0) = 0$, so we must impose a non vanishing initial condition, but it also must be small enough to have no influence on the evolution of the disk, hence we take $T(0) = 1$.

The differential equation (4.34) is a second-order equation, we must therefore impose a boundary condition for both inner and outer parts of the disk. At the inner radius $x = x_{in}$, and from the steady study, we note that all the gas properties are vanishing at this limit, because the orbits are more stable and the matter falls at the central star, so $\Sigma(x = x_{in}) = 0$, we have a boundary condition of type Dirichlet ≪vanishing of the zero derivative≫. This condition does not mean that the mass flux is zero, but the viscous torque is zero [$Pri81$].

Since we will apply this calculation on a binary system, we must take into account that Roch Lobe is the one that determines the outer limit of the disk. At this limit, $x = x_{out}$, the radial velocity $v_r = 0$, and $\frac{\partial \Sigma}{\partial x} = 0$. We have a boundary condition of type Neumann ≪vanishing of the first derivative≫.

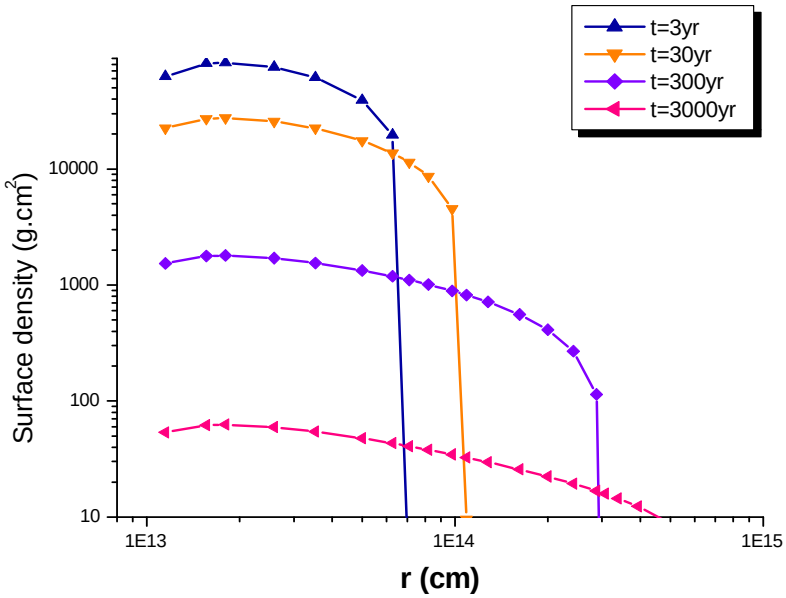

Figure 4.1: The evolution of the surface density in radius and time function.

4.2.5 Time-dependent solutions

The surface density

To complete the set of the constants, we need to know the opacity expression. The observation confirms that the temperature of accretion disks in black hole must exceed $10^4 K$, so we deal with Thomson opacity (2.30),

$$\kappa_0 = 0.34 cm^2 g^{-1} \tag{4.36}$$

where $a = b = 0$. The constant C as a function of viscosity parameter α and according to the above values becomes

$$C = \alpha^{\frac{4}{3}} (10.73)\ cm^{7/3} g^{-2/3} s^{-1} \tag{4.37}$$

From the two equations (4.27) and (4.28), we find that $p = 1$ and $q = \frac{2}{3}$. Therefore, the equations (4.33) and (4.34) become

$$T'(t) + \lambda T^{\frac{5}{3}}(t) = 0 \tag{4.38}$$

and

$$\frac{5}{3}x\,X(x)\frac{\partial^2 X(x)}{\partial x^2} + 10xX(x)\frac{\partial X(x)}{\partial x} + \frac{10}{9}x^2\left(\frac{\partial X(x)}{\partial x}\right)^2 + 6X^2(x) + \frac{\lambda}{C}x^2X^{\frac{4}{3}}(x) = 0 \tag{4.39}$$

Even in time-dependent state, a complete solution of the disk structure requires specifcation of the viscosity, so we need to specify the α value. We have no physical reason for this, and the only known condition is from the researches of Shakura and Sunyaev, which they confirmed that α must be $\alpha \leq 1$. So, we choose the three values 0.01, 0.1, 1.

Now, we solve these equations by the numerical method Runge-Kutta *RK-45* and the computational software program Maple, but first we must put the value of the separation constant λ, we take $\lambda = 10^{-12}$. To illustrate the effect of turbulent viscosity, we fix the time and vary $\alpha = 0.01, 0.1, 1$. The gradual moving of the surface density to the black hole in both space and time function is shown schematically in $(Fig\ 4-1)$.

The plot, from top to bottom, represents the surface density $\Sigma(r,t)$ at times $t = 3, 30, 300, 3000yr$. From these results, we can see that our model of time-dependent thin accretion disks is compatible with $[Can90]$ model. $(Fig\ 4-1)$ shows that at $t = 3yr$, the mass initially orbits in rings at $7 \times 10^{13}cm$, and the maximum surface density $\Sigma_{\max} \simeq 8.2 \times 10^4\ g.cm^{-2}$ in the inner parts of the disk.

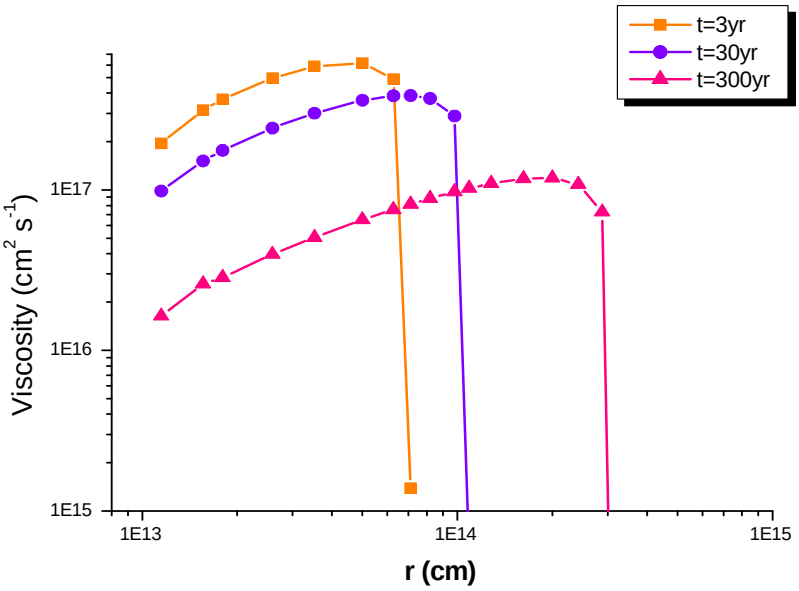

Figure 4.2: The viscosity evolution in function of radius and time.

After $30yrs$, the disk rings spread to outer radius till $1.9 \times 10^{14} cm$, and the surface density decreases. From then on, the rings spread out with time even up to a radius of order $7.96 \times 10^{14} cm$ after $3000yrs$. This means that the matter moves to the outer parts of the disk.

As the accretion process proceeds, the matter that falls onto the disk tends to rotate around the star in stable orbits, because it has enough angular momentum. As we said before that in this calculation, we neglect the effect of self-gravity of the disk and do not bear in mind the magnetic field, so the only effective mechanism that can extract the angular momentum from the particles to accrete is the turbulent viscosity. The following results of the viscosity ($Fig\ 4-2$) show the large values of it, up to $6 \times 10^{17} cm^2.s^{-1}$.

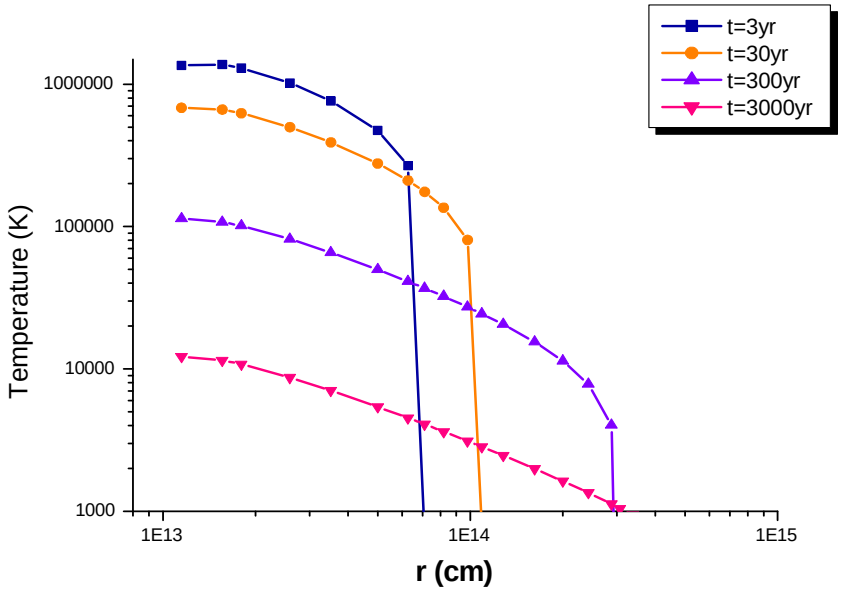

Figure 4.3: The evolution of the temperature in both radius and time.

The temperature

From the temperature equation (4.23), we find

$$T = \frac{C}{\alpha}(2.71 \times 10^8)\Sigma^{2/3}\ r^{-1/2} \tag{4.40}$$

Substituting with the previous surface density solution to design the evolution of T with radius and time.

The plot $(4-3)$ gives the radial distribution of temperature $T(r,t)$ with times $t = 3, 30, 300, 3000yr$, our results are in good agreement with $[Can90]$, but the unique difference is the maximum value of T. The plot illustrates that the same general features with the surface density Σ are shown by the changes of T.

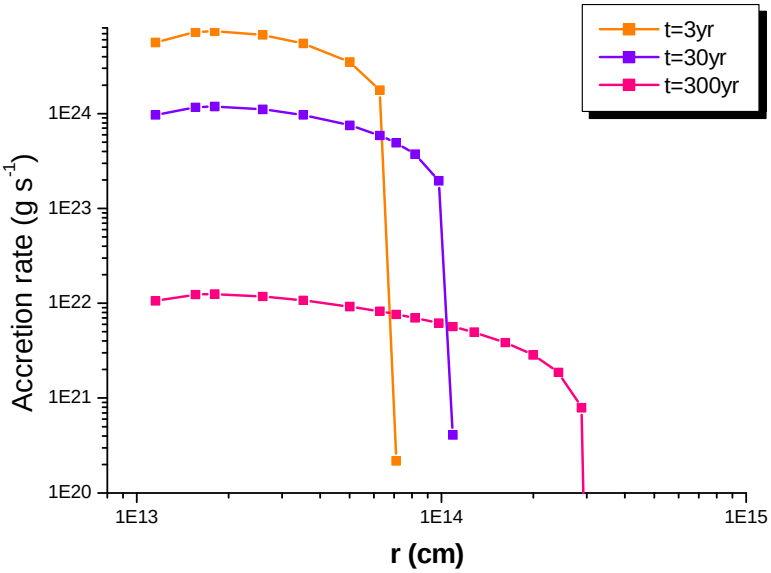

Figure 4.4: The evolution of the accretion rate in function of both radius and time.

Once the accretion onto the black hole has started, the temperature exhibits a rapid rise to $T \sim 1.37 \times 10^6 K$, and continues to increase as the particles move toward the innermost regions of the disk, where most of the energy releases. This increase of temperature arises because when the disk particles move toward the central star, due to their loss of the angular momentum, they lose their gravitational energy too, this energy heats the disk to be emitted as a radiation. Also, the shocks experienced by the disk particles raise its temperature. Then, temperature decreases and the disk becomes cool with time.

The accretion rate

The accretion rate is given by the integral

$$\dot{M}= \frac{\dot{dm_{disk}}}{dt}= \int_{r_{in}}^{r_{out}} 2\pi r \frac{d\Sigma}{dt} dr \tag{4.41}$$

thus

$$\dot{\dot{M}}= \frac{dT(t)}{dt} \int_{r_{in}}^{r_{out}} 2\pi r X(x) dr \tag{4.42}$$

It is important to calculate the accretion rate because it is used to determine the disk luminosity. $(Fig\ 4-4)$ shows the evolution of the rate $\dot{M}$ in both position and time function, the values of $\dot{M}$ in the range of 8.2×10^{19} to $7.38 \times 10^{24} g.cm^{-1}$. Many calculations have been completed in order to get an estimation for the tidal disruption rate [$Ree88$], the result was that for $M32$, our galaxy and other nearby galaxies is $M \sim 10^{19} - 10^{20} g.cm^{-1}$. The range of our accretion rate solution exceeds these values, which confirms the tidal disruption efficiency of stars near a $10^7 M_\odot$ black hole.

The total disk luminosity L_{disk}

Using the above temperature solution to represent the luminosity solution in $(Fig\ 4-5)$. From this curve, we find the range of luminosity in disks around the supermassive black hole, from 1.4×10^{39} to $3 \times 10^{44} erg.s^{-1}$. Accretion disks in this case are considered as a big source of energy due to the large amount of luminosity that they can release, where half of this gravitational energy converts into thermal energy to radiate from the disk surface mainly in ultraviolet and X-ray bands [$Sha73$], and the other half increases the kinematic energy of rotation. This large amount of luminosity can not escape from the disk without affecting

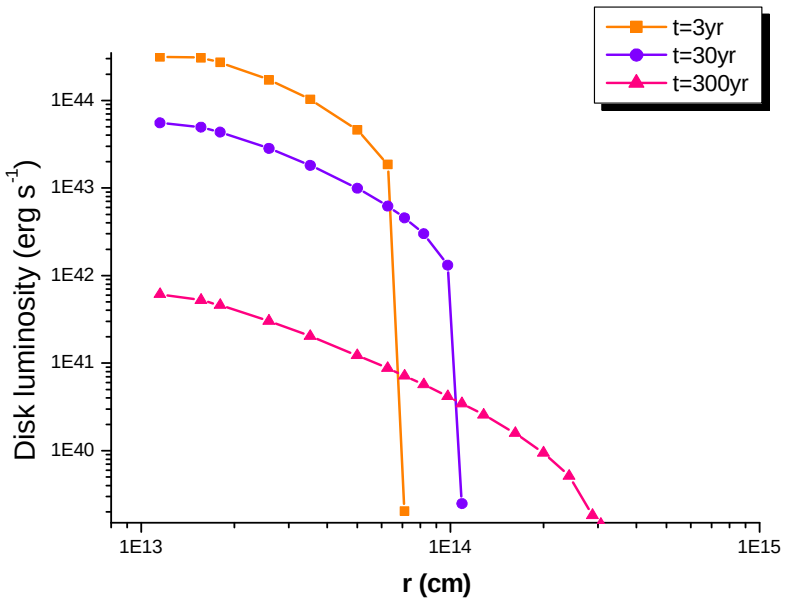

Figure 4.5: The evolution of the disk luminosity as a function of both radius and time.

the black hole, the neighbouring stars or the disk itself. In close binary systems, a part of this radiation can reach the surface of the companion star, to radiate by its atmosphere, this leads to an unusual optical appearance in this system, such as that observed in the binary HZ Her / Her X-1.

The extraction of this gravitational energy releases with a radiative efficiency

$$\eta = \frac{L}{\dot{M}\ c^2} \simeq 0.04 \tag{4.43}$$

η represents the efficiency with which the rest mass of the accreted material can be transformed into radiation. The value $\eta \simeq 0.04$ is supported by $[Sha73]$ for disks around non rotating supermassive black holes, and it means that the disk in this case can convert and emit up to 4% of its accreted rest mass as radiation. This radiative efficiency depends on the magnetic field strength, we can find larger values if we take the effect of magnetic field (the real case), up to $\eta = 4$, which distinguishes the case of a rotating or Kerr balck holes. The study of this type of holes demonstrates that the accretion around a black hole is the most efficient way of transforming gravitational potential energy into radiation.

The critical value of the luminosity is determined by the Eddington limit, The value of this limit for a black hole of mass $10^7 M_\odot$ is

$$L_{edd} = 1.3 \times 10^{38} \left(\frac{M}{M_\odot}\right) erg.s^{-1} = 1.3 \times 10^{45} erg.s^{-1} \tag{4.44}$$

Hence, the luminosity values of this solution are approach to this limit especially in the early phase of disk evolution, and this is due to the large viscous stress in accretion disks formed from stellar debris, that are made to keep the luminosity

close to Eddington limit, then it begins decreasing, thus our values are correct as long as they are less than L_{edd}. For this, the Eddington limit is a necessary condition to the validity of thin approximation. Also we can define the critical accretion rate as

$$\dot{M}_{crit} = \frac{12}{c^2} L_{edd} \simeq 1.73 \times 10^{25} g.s^{-1} \tag{4.45}$$

4.3 Results and outlooks

Here we built a model of time-dependent accretion disk by assuming that the disk is geometrically thin and optically thick, and we compared it with [$Can90$], the results are supported with the curves. This time-dependent study is considered as one of the most important sources of quantitative information about the disk properties.

This study confirms that the accretion process provides a huge source of energy, and the time dependence of disk flow is controlled by the size of the viscosity, where the viscous dissipation is necessary to transport angular momentum, it will also heat the gas where this heat can be radiated away or advected inward with the accreting gas.

In order to accrete gas, its particles must move inward from orbit to another by losing their angular momentum and gravitational energy. Since total angular momentum must be conserved, other gas particles must gain angular momentum and move outward, this leads to spread out the disk structure.

The viscous timescale is the required time for the particles to diffuse through the disk under the effect of the viscous torque, it is inversely dependent on the

change of viscosity. In the outer regions of the disk, the viscosity suddenly rises, the viscous timescale is short and the matter rapidly accretes (low surface density). In the inner regions, the viscosity decreases, so the viscous timescale is long, which allows the matter to accumulate in this region (high surface density). This increase in the surface density explains the high luminosity in the inner regions, because it leads to raise the disk temperature that becomes unstable.

Conclusion and perspectives

To understand the structure of an accretion disk, we must follow the motion of the particles that fall onto it from large to small radius. The numerical simulation shows that the viscosity is one of the main agents responsible for this transport.

In this thesis, we have studied the structure and properties of accretion disks that are formed around stellar objects, with using the concept of turbulent viscosity "α-disk model" in the two cases; steady and time-dependent state.

We have begun by studying the steady solution of geometrically thin disks around white dwarfs; this study has provided good information about the shape and the properties of the disk. Since the case of thin disks is more theoretical than realistic, we have imposed a model that describes the geometrically thick disks, and we have solved the equations of this model to get more information about the structure of the disk in this case.

In this thesis, we have tried to find solutions to the following questions

* What happens if the disk viscosity is not constant?

* Can turbulent viscosity proposed by standard model drive the mass transport

in accretion disks?

* What happens if the disk is not thin?

* What happens if the gas in an accretion disk does not follow Keplerian orbits?

In order to answer the previous questions, we have proposed a new solution of time-dependent thin accretion disks, with using the α-prescription of the viscosity. We have obtained results supported with the experimental observations and other models.

There are several reasons for extending the steady study to time-dependent one. The most important is that the observable properties of the disk are almost independent of the viscosity, and do not give much information about the disk viscosity, while the time-dependent hydrodynamical study that has been presented in chapter four, clearly shows that the evolution of the disk with time is strictly dependent of the viscosity size.

The question that still arises for this study is: what is the physical origin of turbulence and viscosity in accretion disks? Other mechanisms might be important in carrying angular momentum, and giving more information about the source of viscosity. The most promising possibility at present is the one that depends on the magnetic instability or that well known by MHD. There are number of available numerical codes to simulate this instability, but they all need powerful computers. Our next perspective is the study of magnetorotational instability in accretion disks and the use of one of the previous codes that have been mentioned in chapter one.

bibliography

[And07] Nils Andersson, G. L. Comer, Relativistic fluid dynamics: physics for many different scales, Living reviews in relativity, 2007.

[Arn62] R. Arnowit, S. Deser, W. Misner, Gravitational: An introduction to current research. New York: Wiley, 1962.

[Art09] G. A. Articolo, Partial differential equations and boundary value problems with Maple, Elsevier press, 2009.

[Bal96] Steven A. Balbus, J. F. Hawley, Instability, turbulence, and enhanced transport in accretion disks, Review of Modern Physics, 1998.

[Bal03] Steven A. Balbus, Enhanced angular momentum transport in accretion disks, arXiv: astro-ph/0306208v1.10 Jun 2003.

[Bat81] G. T. Bath & J. E. Pringle, The evolution of viscous discs- I: Mass transfer variation, Mon. Not. R. Astr. Soc. 194: 967-986, (1981).

[Cal99] Nuria Calvet & Lee Hartmann, Evolution of disk accretion, arXiv: astro-ph/9902334v1.23 Feb 1999.

[Can90] John K. Cannizzo & Hyung Mok Lee & Jeremy Goodman, The disk accretion of a tidally disrupted star onto a massive black hole, The astrophysical journal, 351: 38-46, 1999.

[Cla07] C. J. Clarke & R. F. Carswell, Principles of astrophysical fluid dynamics, Cambridge university press, 2007.

[Clar01] A. Claret, A. Giménez, Physical processes in close binary systems, LNP 563, pp . 1-47, 2001.

[Del02] A. Del Popolo & K. Y. Eksi, Migration of giant planets in a time-dependent planetesimal accretion disc, arXiv: astro-ph/0201320v1.18 Jan 2002.

[Dur08] F. Durst, Fluid Mechanics, An introduction to the theory of fluid flows, Springer, 2008.

[Fra02] J. Frank, A. King, D. Raine, Accretion power in astrophysics, Cambridge University press, 2002.

[Gou06] E. Gourgoulhon, An introduction to relativistic hydrodynamics, arXiv: gr-qc/0603009 v1 5Mar 2006.

[Har06] Martin Harwit, Astrophysical concepts, Springer, 2006.

[Hart06] Lee Hartmann, Accretion Processes In Star Formation, Cambridge University Press, 1997.

[Haw97] J. F. Hawley & S. A. Balbus, Three-dimensional simulations of accretion disks, ASP Conference Series, 121: 179-189, 1997.

[Hor04] G. P. Horedt, Polytropes applications in astrophysics and related fields, Kluwer Academic publishers, 2004.

[Lan87] L. D. Landau and E. M. Lifshitz, Fluid Mechanics, Pergamon Press, 1987.

[Liv91] M. Livio, H. C. Spruit, On the mechanism of angular momentum transport in accretion disks, Astron. Astrophys. 252, 189-192, 1991.

[Lu00] Y. Lu, K. S. Cheng, L. T. Yang & L. Zhang, A massive thick disc around a massive black hole and its runaway instability, Mon. Not. R. Astron. Soc. 314, 453-458, 2000.

[Lyn74] D. Lynden-Bell & F. E. Pringle, The Evolution Of Viscous Discs And The Origin Of The Nebular Variables, Mon. Not. R. astr. Soc, I68: 603-637, 1974.

[Pac80] B. Paczynski, A model of a thick disk with a surface accretion layer, Acta Astronomica, 30: 347-363, 1980.

[Pap95] J. C. B. Papaloizou & D. N. C.Lin, Theory of accretion disks I: Angular momentum transport processes, Annu. Rev. Astron. Astrophys. 33:505-40, 1995.

[Pri81] J. E. Pringle, Accretion discs in astrophysics, Ann. Rev. Astron. Astrophys, 19:137-162, 1981.

[Pri72] J.E. Pringle & M. J. Rees, Accretion disc models for compact X-ray sources, Ann. Rev. Astron. Astrophys, 21:1-9 , 1972.

[Ree88] M. J. Rees, Tidal disruption of stars by black holes of 10 to the 6th-10 to the 8th solar masses in nearby galaxies, Nature, 333: 523-528, 1988.

[Reg08] Oded Regev, Hydrodynamical activity in thin accretion disks, New Astronomy Review 51. 819-827, 2008.

[Ric06] W. K. M. Rice, G. Lodato, J. E. Pringle, P. J. Armitage, I. A. Bonnell, Planetesimal formation in self- gravitating protoplanetary discs, Mon. Not. R. Astron. Soc. 372, L9-L13 (2006).

[Rub05] E. Rubio-Herrera & W. H. Lee, Oscillations of thick accretion discs around black holes, Mon. Not. R. Aston. Soc. 357, L31-L34 (2005).

[Sha73] N. I. Shakura & R. A. Sunyaev, Black holes in binary systems. Observational appearance, Astron. & Astrophys. 24, 337-355, 1973.

[Shi07] I. Shingareva & C. Lizàrraga-Celaya, Maple and Mathematica, Springer

Wien New York, 2007.

[Sow02] A. M. Soward & C. A. Jones & D.W. Hughes & N. O. Weiss, Fluid dynamics and dynamos in astrophysics and geophysics, CRC Press, 2002.

[Spu08] Joseph H. Spurk & Nuri Aksel, Fluid mechanics, Springer, 2008.

[Yam08] H. Yamaguchi, Engineering fluid mechanics, Springer, 2008.

[Zur86] W. H. Zurek & W. Benz, Redistribution of angular momentum by non axisymmetric instabilities in a thick accretion disk, The astrophysical journal, 308: 123-133, 1986.